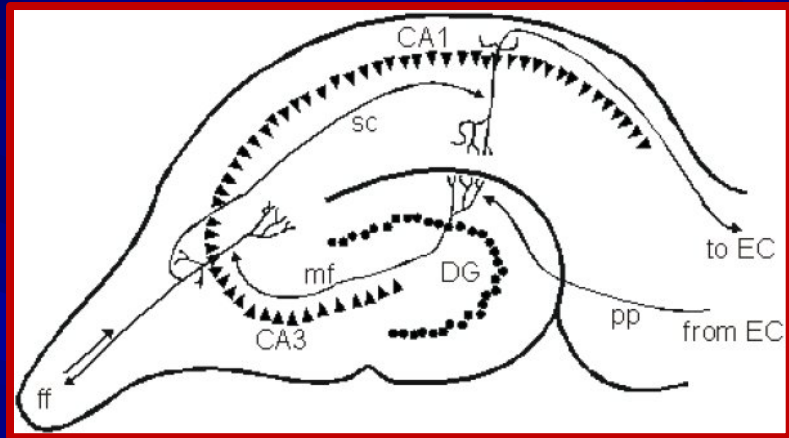
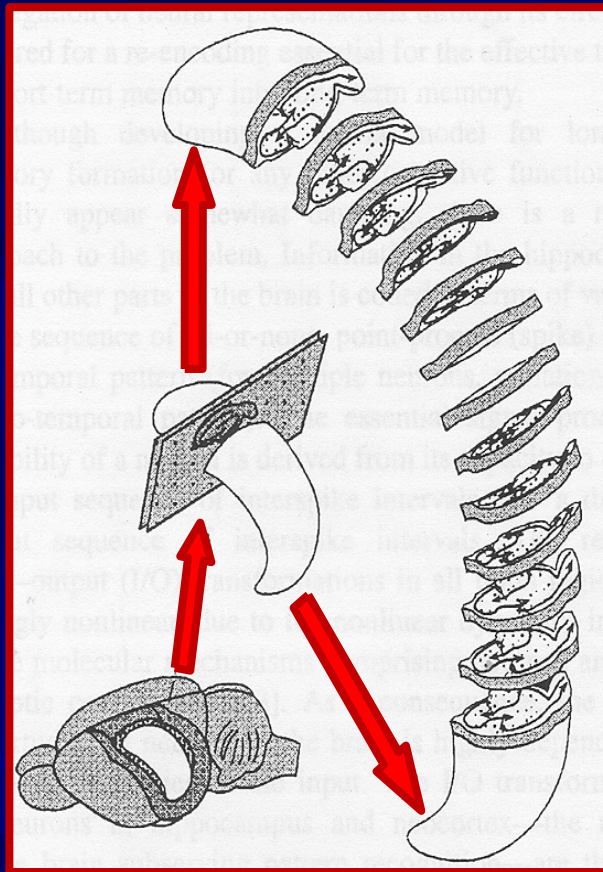
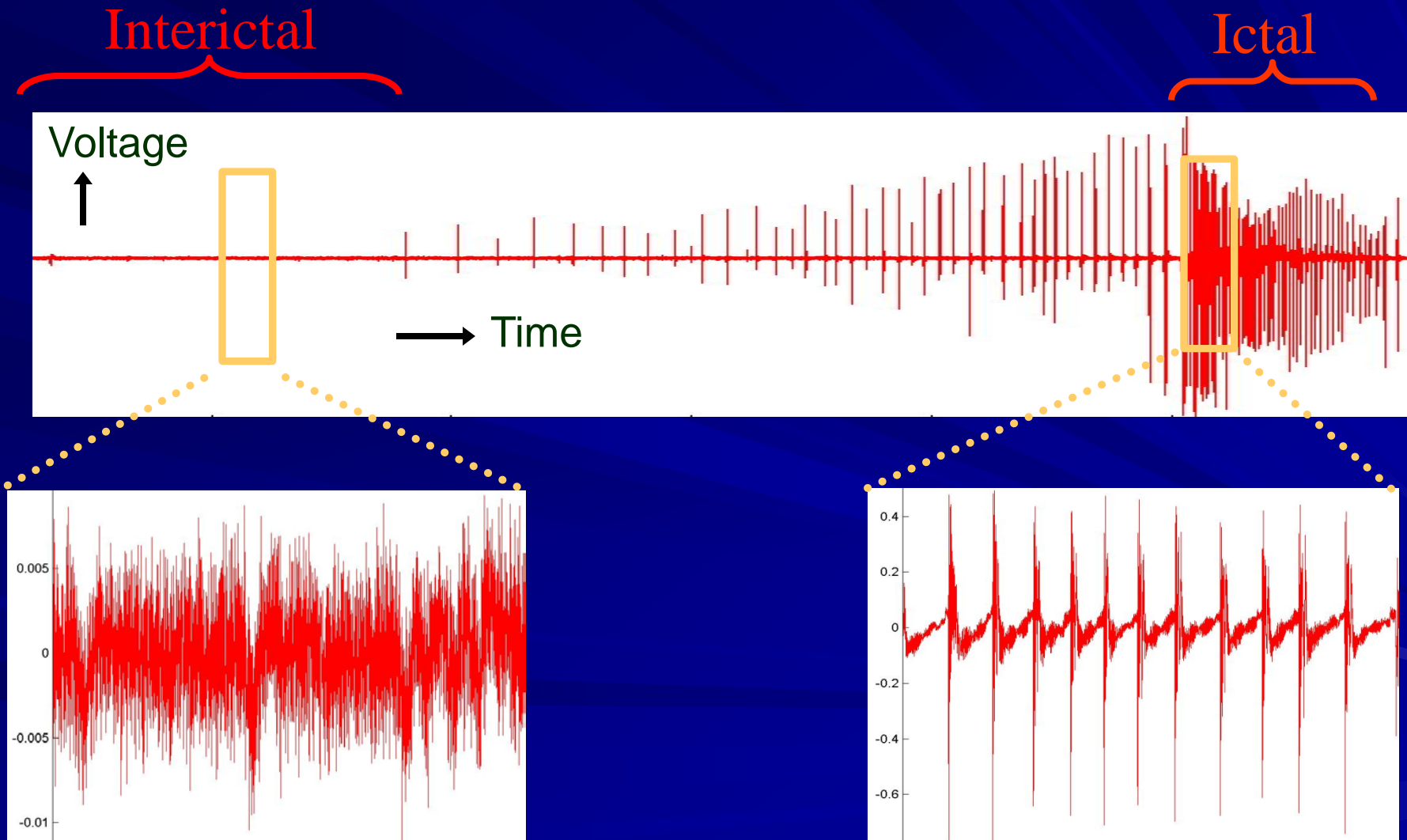


Seizure-Like Events (SLEs) in Rodent Models

Low Mg²⁺ High K⁺ in-vitro model of Spontaneous SLEs



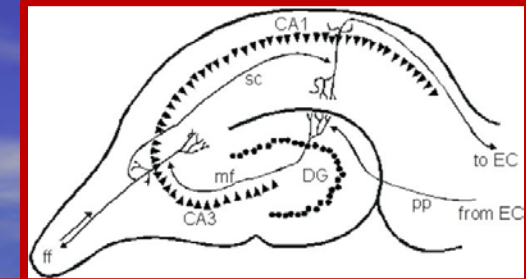
Low Mg^{2+} High K^+ in-vitro model of Spontaneous SLEs



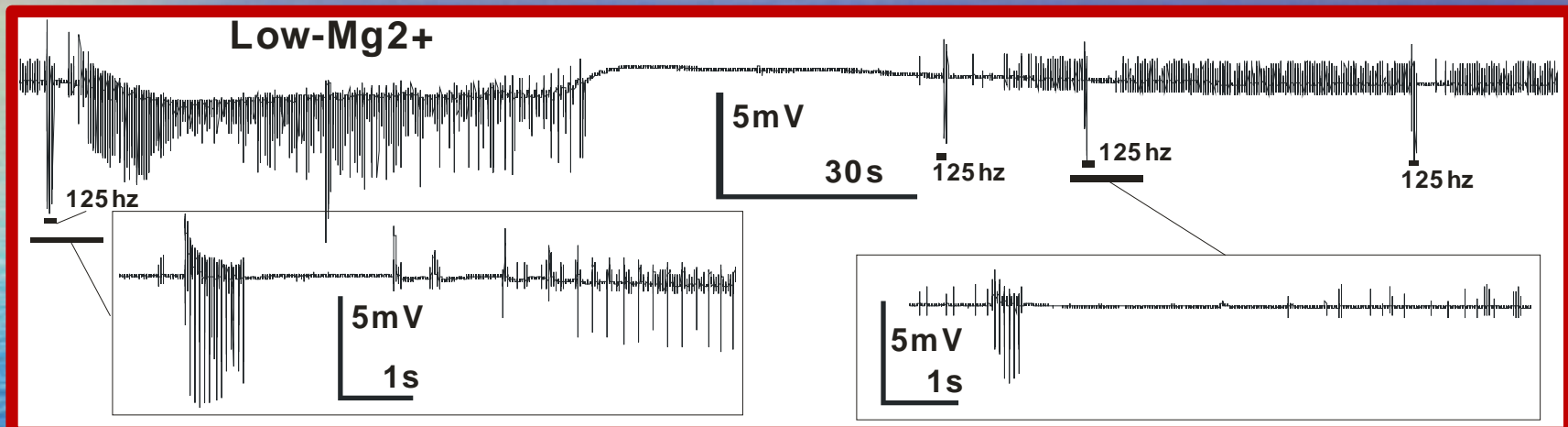


Brain stimulation strategies to stop seizures

Low-Mg²⁺ model: High frequency (125 Hz) stimulation



Mossy fibre stimulation, CA1 recording



1 s of 125 Hz stimulation failed to control seizure

0.3 s of 125 Hz stimulation prevented further development into seizure

High frequency periodic stimulation only transiently blocks seizures.
This is what is presently being used for deep brain stimulation, with very limited success in epilepsy.

Seizure Suppression Efficacy of Closed-loop Versus Open-loop Deep Brain Stimulation in a Rodent Model of Epilepsy

M. Tariqus Salam, *Member, IEEE*; Jose Luis Perez Velazquez;
Roman Genov, *Senior Member, IEEE*

ARTICLE in IEEE TRANSACTIONS ON NEURAL SYSTEMS AND REHABILITATION ENGINEERING · JANUARY 2015

Impact Factor: 3.19 · DOI: 10.1109/TNSRE.2015.2498973

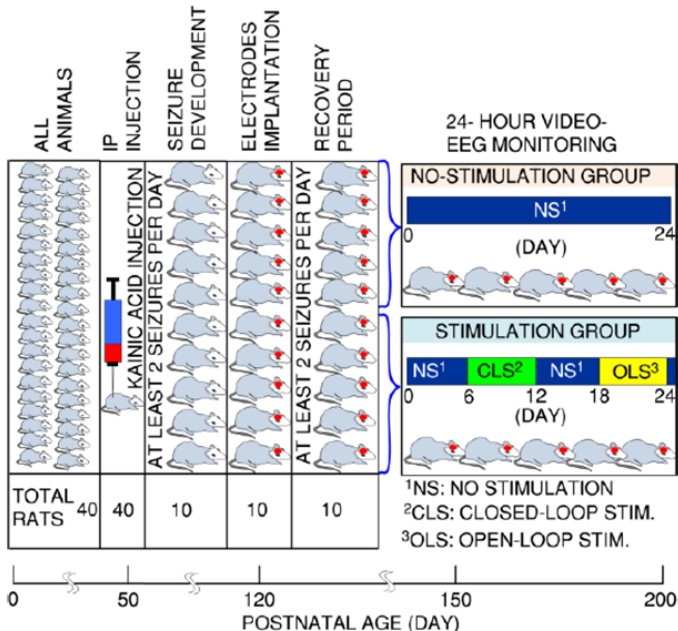


Fig. 2. Experimental procedure: 40 male Wistar rats were used in this study. Kainic acid was injected into the rats at their 50-day age and after ~60 days of injection, 10 rats were developed spontaneous seizure. All seizure induced rats were anesthetized for electrode implantation around their 120-day age. Later these rats were randomly divided into two groups to evaluate the seizure suppression efficacy. The no-stimulation group went through the 24-hr video EEG monitoring, but the stimulation group had four experimental phase (each phase was 6 days long).

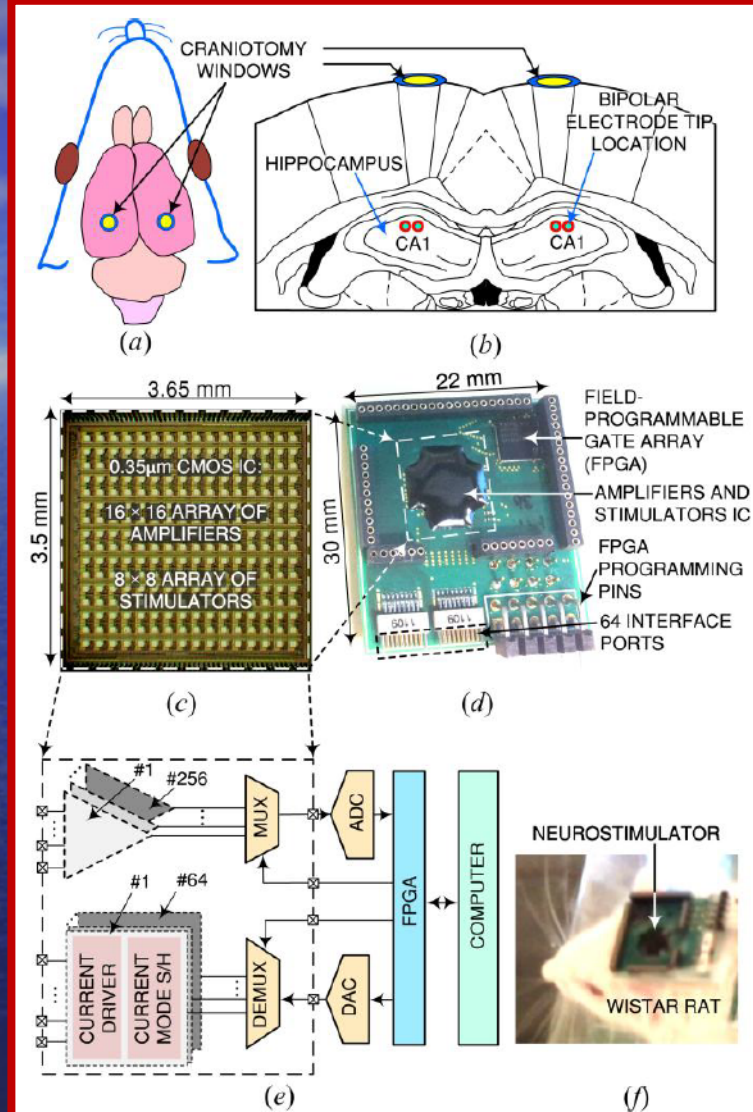


Fig. 3. Bipolar electrode implantation: (a) - (b) locations of craniotomy windows and implanted electrode tips. (c) Bi-directional neural interface custom integrated circuit with 256 neural amplifiers and 64 neurostimulators, (d) custom-made programmable therapeutic neurostimulation device with 64 recording channels or 64 stimulation channels enabled, (e) system-level block diagram, and (f) a freely moving rat with the neurostimulator mounted on the head to demonstrate the form factor.

Rapid brief feedback intracerebral stimulation based on real-time desynchronization detection preceding seizures stops the generation of convulsive paroxysms

*Muhammad T. Salam, *Hossein Kassiri, *Roman Genov, and †Jose L. Perez Velazquez

Epilepsia, **():1–12, 2015

doi: 10.1111/epi.13064

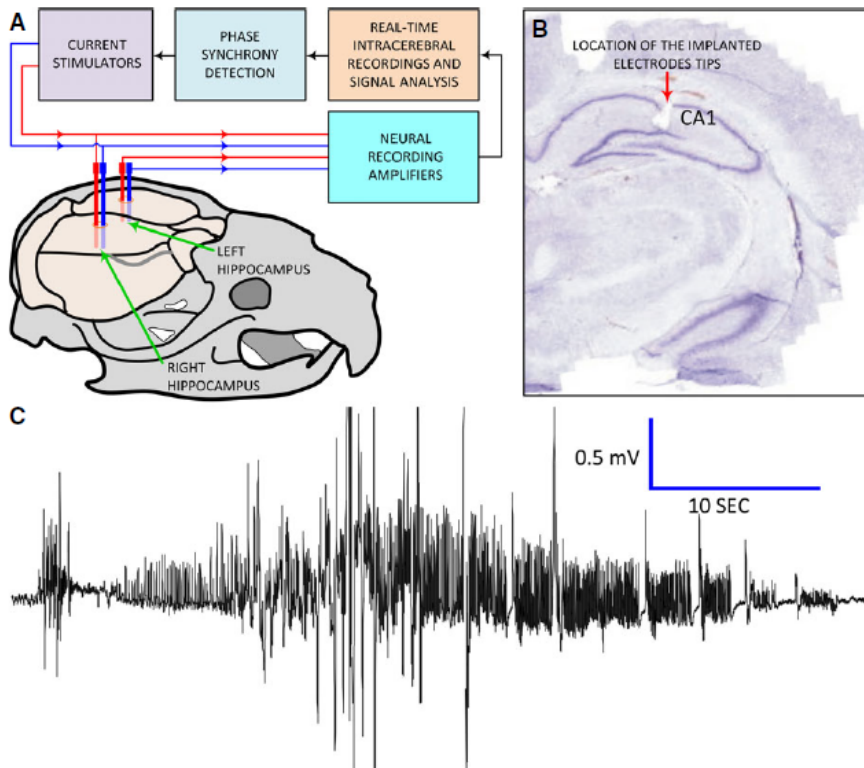


Figure 1.

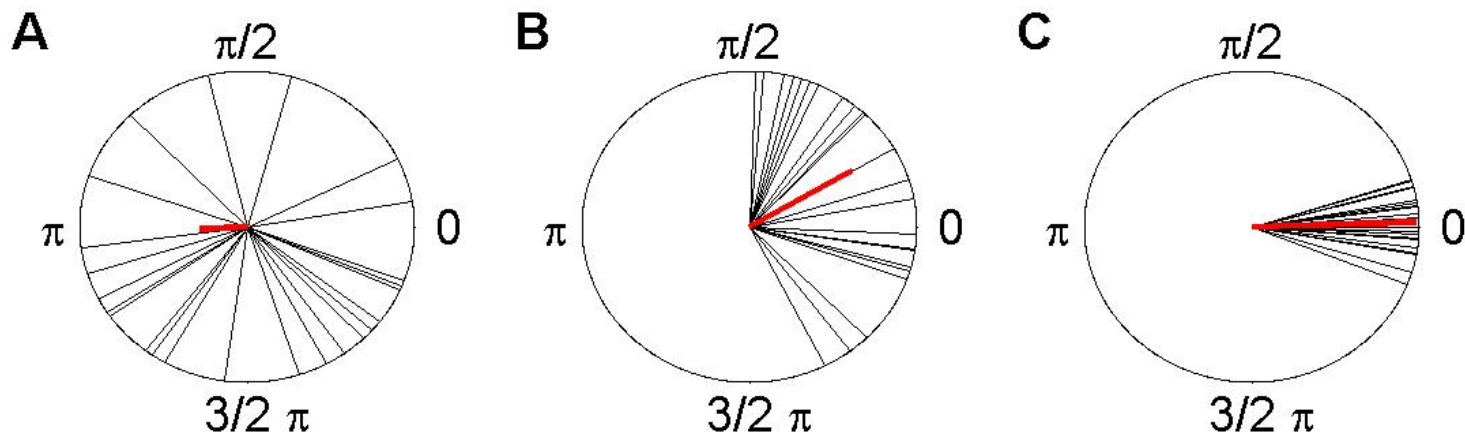
(A) General scheme of our methodology. (B) A cresyl-violet stained brain section showing the location of the implanted electrode tips. (C) Representative example of a spontaneous paroxysm in the chronic condition (>2 months after kainate injection).

Epilepsia © ILAE

Neuronal Phase Coherence (or Synchrony) Index “R”

$$R = \left| \frac{1}{N} \sum_{j=1}^N e^{i[\phi_x(t_j) - \phi_y(t_j)]} \right|$$

$\phi_x(t)$ and $\phi_y(t)$ are the phase time series obtained from either the complex Wavelet Transform or the Hilbert Transform



Index of phase synchronization based on circular variance.
Distribution of phase differences and mean phase difference (in red) for
A. uncorrelated, B. weakly correlated, and C. strongly correlated time series.

Seizure precursor detection in the chronic condition.

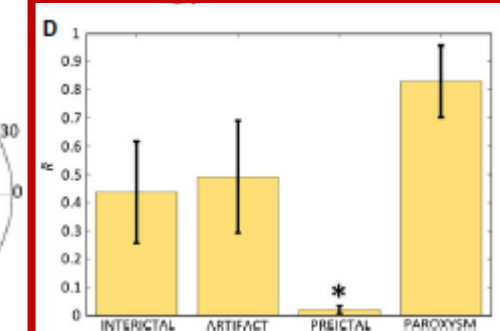
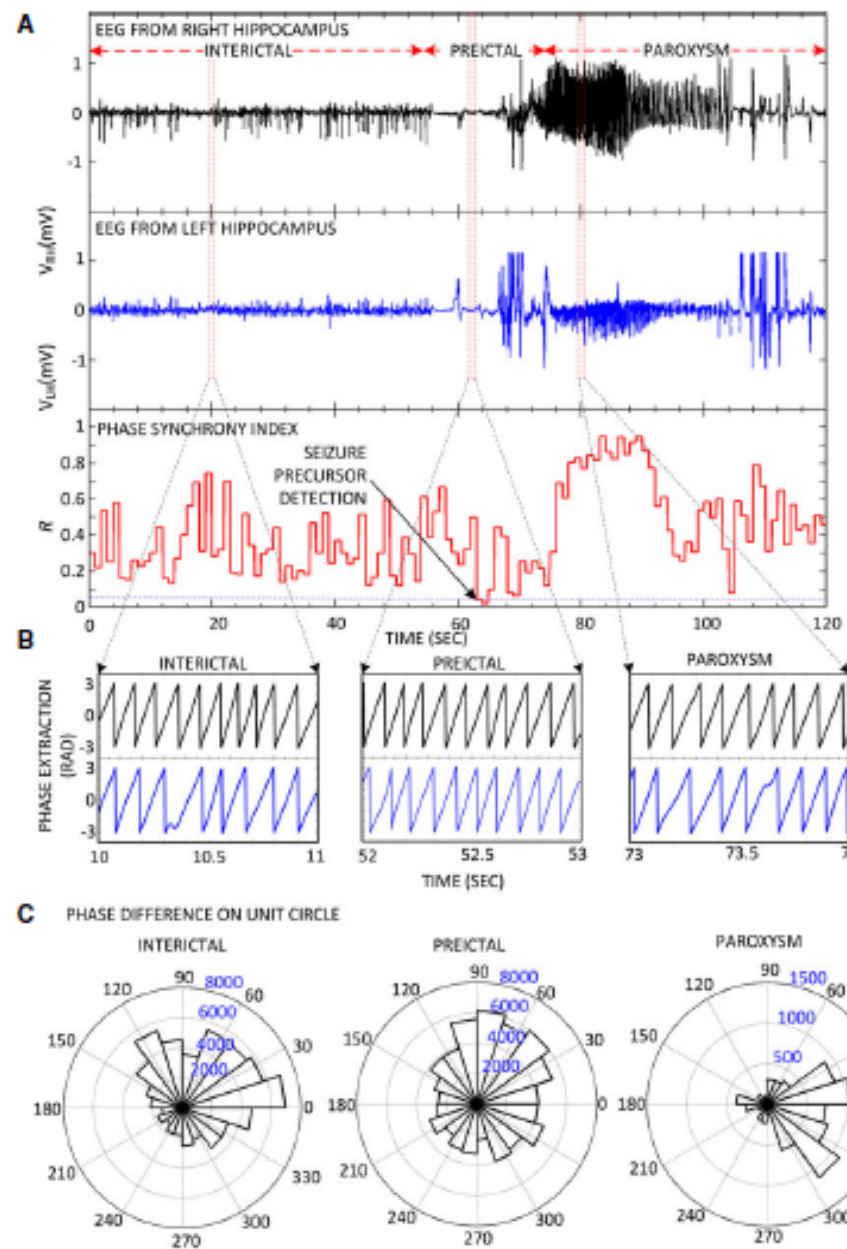
(A) Detection is indicated when synchrony index R, evaluated at central frequency of 8 Hz, is below the threshold of 0.05 (marked by the solid arrow) for a “nonstimulation group” rat. Upper traces are recordings from both hippocampi showing the paroxysm approximately from the time period 70–100 s; the lower graph is the time evolution of the R index. The high R value is noticed during most of the paroxysm.

(B) Phase extraction from interictal, preictal, and ictal periods in both hippocampal signals, that were used to compute the synchrony index, the typical sawtooth shape can be seen in all three segments.

(C) The phase differences on the unit circle. More dispersed distribution of angles occurs during preictal state, which translates into a lower R index.

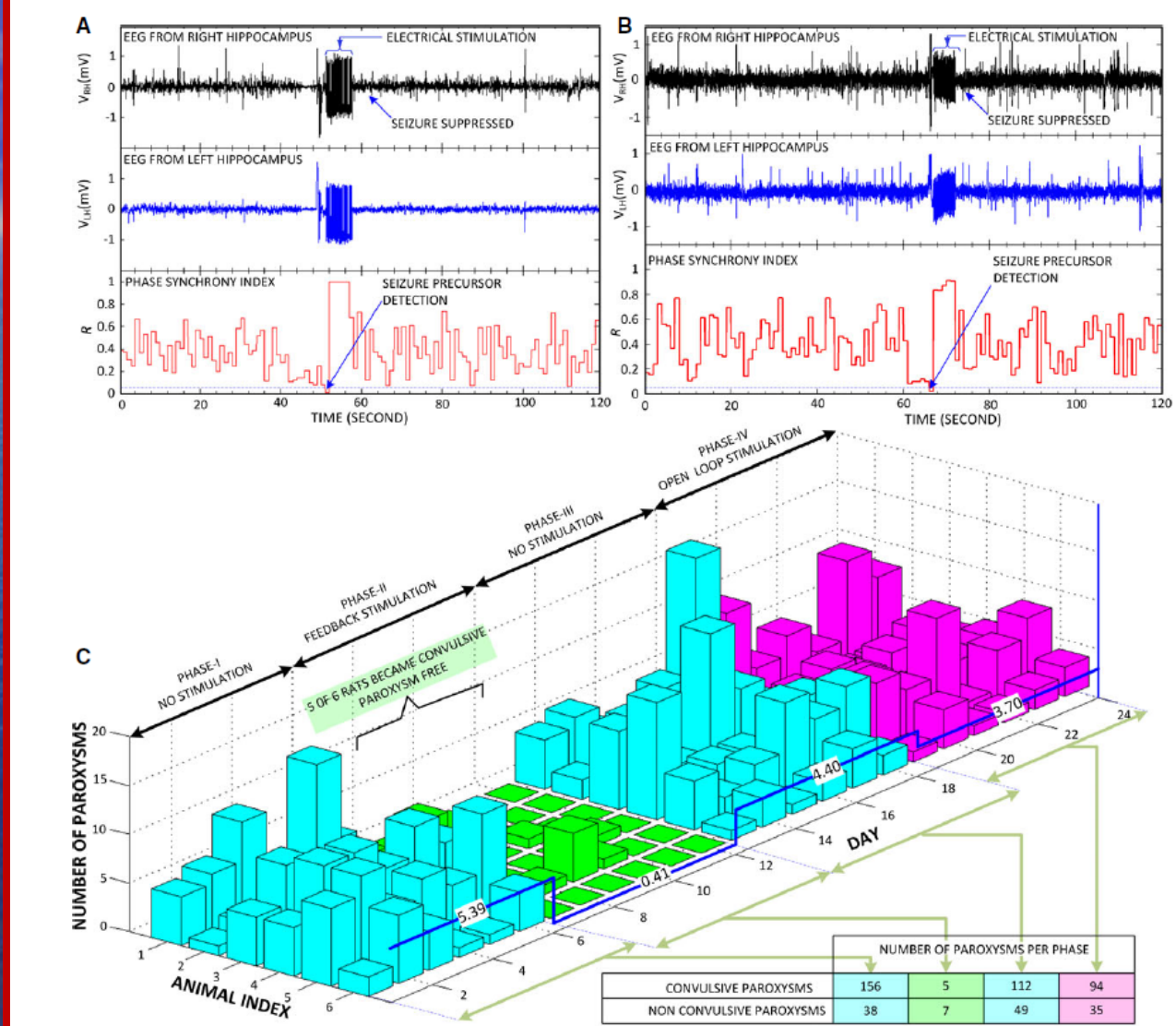
(D) Average of the “R” evolution between the two hemispheres during interictal, artifact, preictal & paroxysmal periods. R drops significantly during the preictal period ($*p < 0.05$).

“Artifact” denotes rat movement (confirmed by video).



Representative examples of seizure suppression by the feedback electrical stimulation for a rat in the stimulation group of chronic (A) and acute (B) models. After the R index falls below the predefined threshold (denoted by the discontinuous line in third row), the feedback system triggers the stimuli and no paroxysmal event follows, and there is no increase in the “R” characteristic of seizures. The high value of “R” in A and B was due to the 5 s stimulation artifact.

(C) Seizure suppression results in the chronic condition. During the 6 days of the no-stimulation phase I, ~5.39 seizures per day on average were observed. The stimulation phase II reduced seizure rate to 0.41, and another no stimulation phase (phase III) yielded ~4.40 seizures per day. The open-loop stimulation phase presented on average 3.70 seizures per day. The table inset indicates number of convulsive and nonconvulsive paroxysms.



Prediction of antiepileptic drug treatment outcomes using machine learning

Sinisa Colic¹, Robert G Wither³, Min Lang², Liang Zhang⁴,
James H Eubanks⁵ and Berj L Bardakjian⁶

Experimental Setup

Model

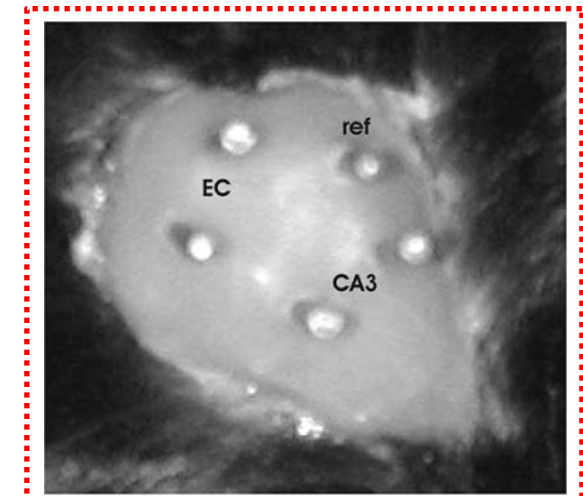
- Mecp2-deficient female C57Bl/6 mice (n=6) over five age periods (3, 5, 8 , 14 and 19 months) and after ACD treatments
- *Mecp2* gene reactivated (rescue) mice (n=4)

Data Acquisition

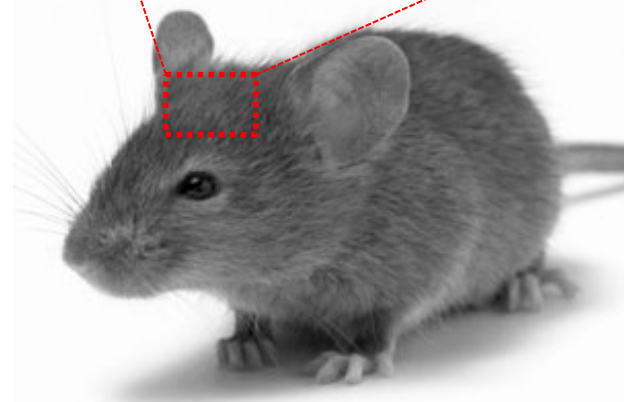
- wired *in vivo* recordings obtained from parietal cortex
- reference implanted in the frontal brain region
- 0.5-1 hours of recording
- 60 kHz sampling

Preprocessing

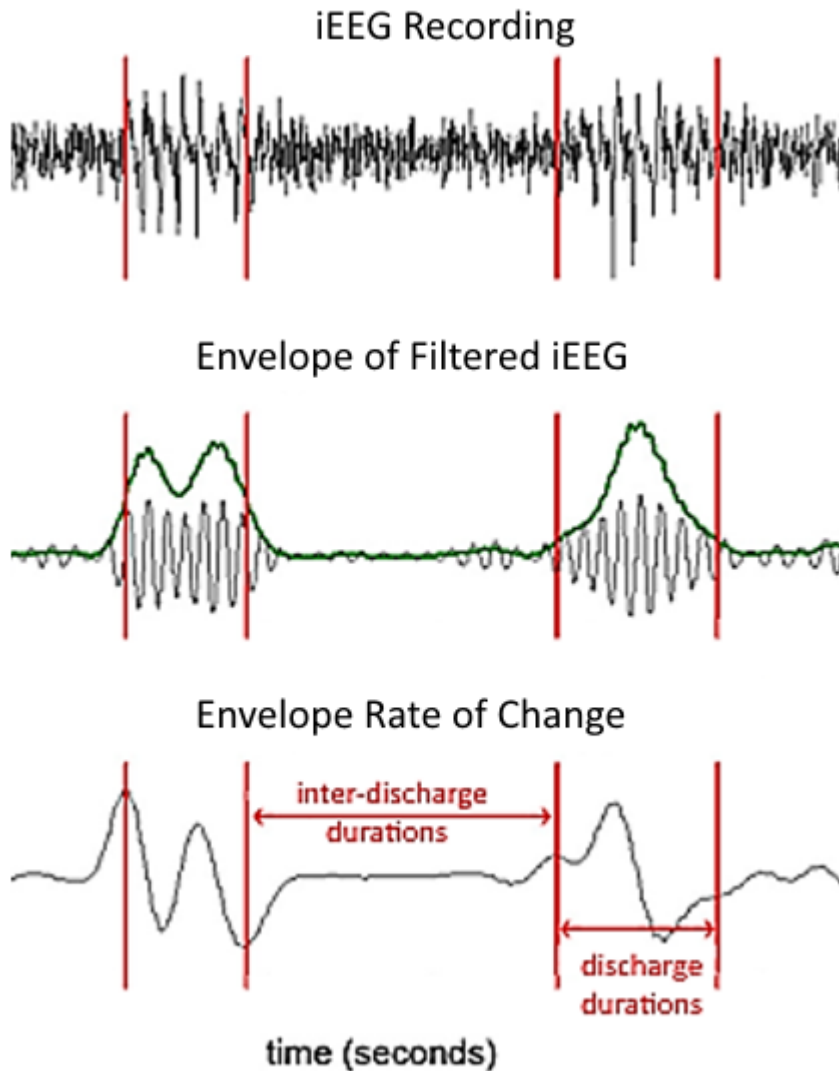
- 60 Hz line noise removal
- large amplitude muscle artifact segments excluded
- data were downsampled to 4 kHz



Wu et al., 2009



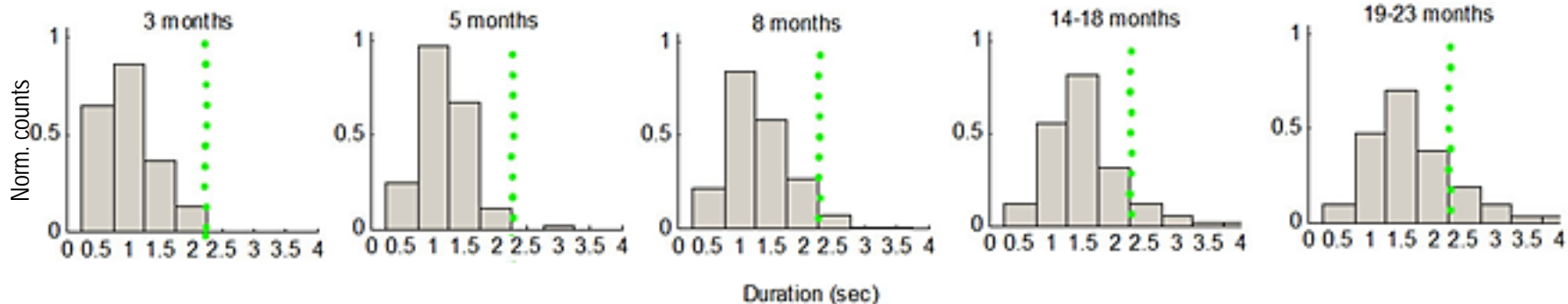
Estimation of Discharge Durations



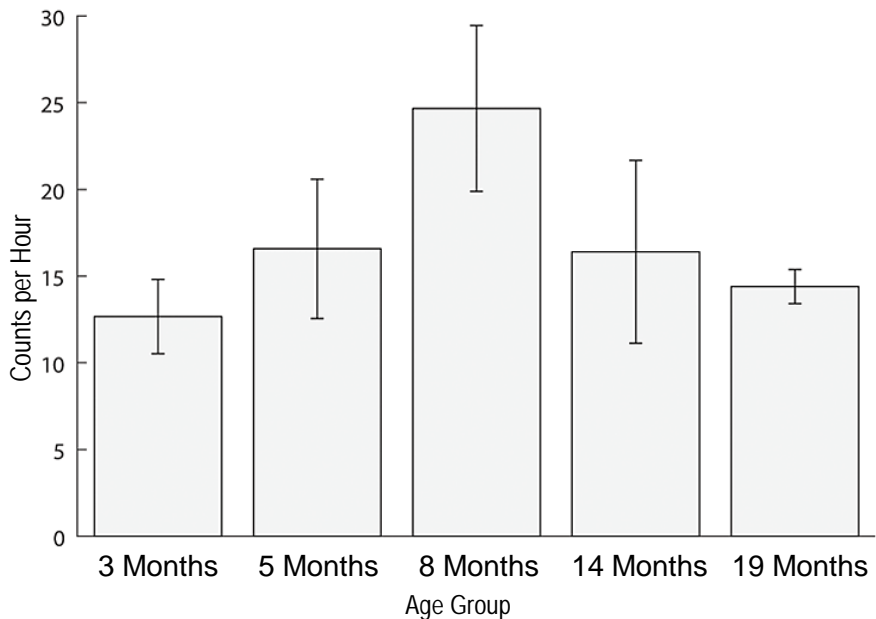
- Mecp2-deficient mice show electrical discharges
- Hundreds of discharges over many hours of recordings requires **automated detection**
 - 6 – 10 Hz bandpass filter
 - Power threshold used to select candidate discharges
 - Inflection points used to indicate discharge start and end time

Discharge Durations

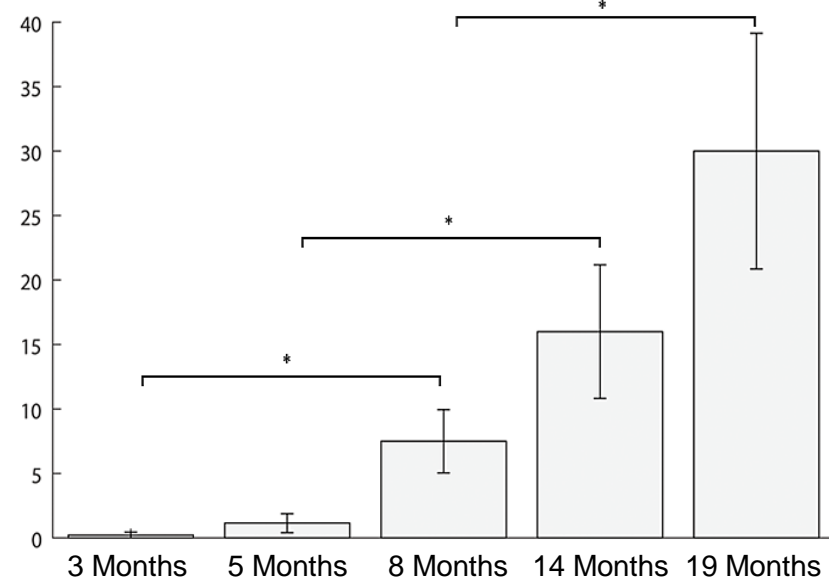
Long duration discharge increase tracks discharge pathology



Short Duration Discharges (<2sec)

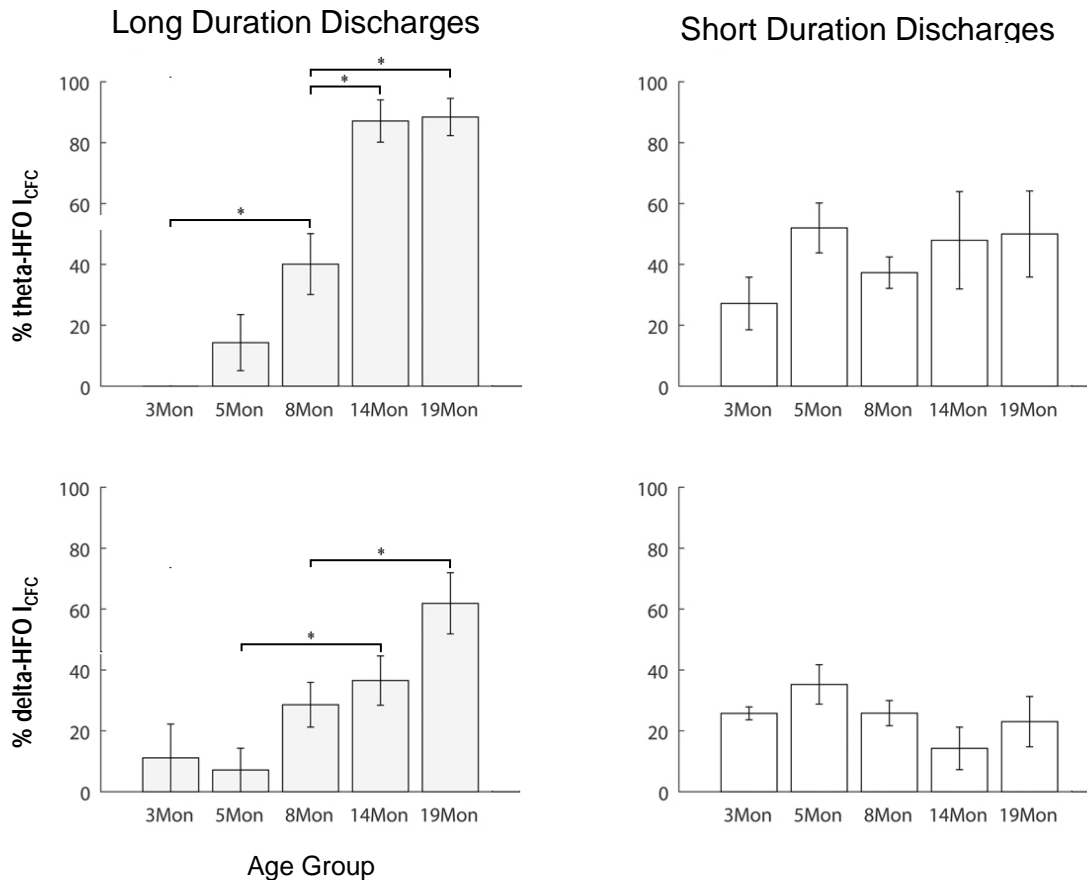


Long Duration Discharges (>2sec)



Tracking LFO-HFO I_{CFC}

- Percentage of theta-HFO and delta-HFO I_{CFC} in long duration discharges increases with age of subjects
- No significant change observed in the short duration discharges



Mecp2 Gene Reactivation

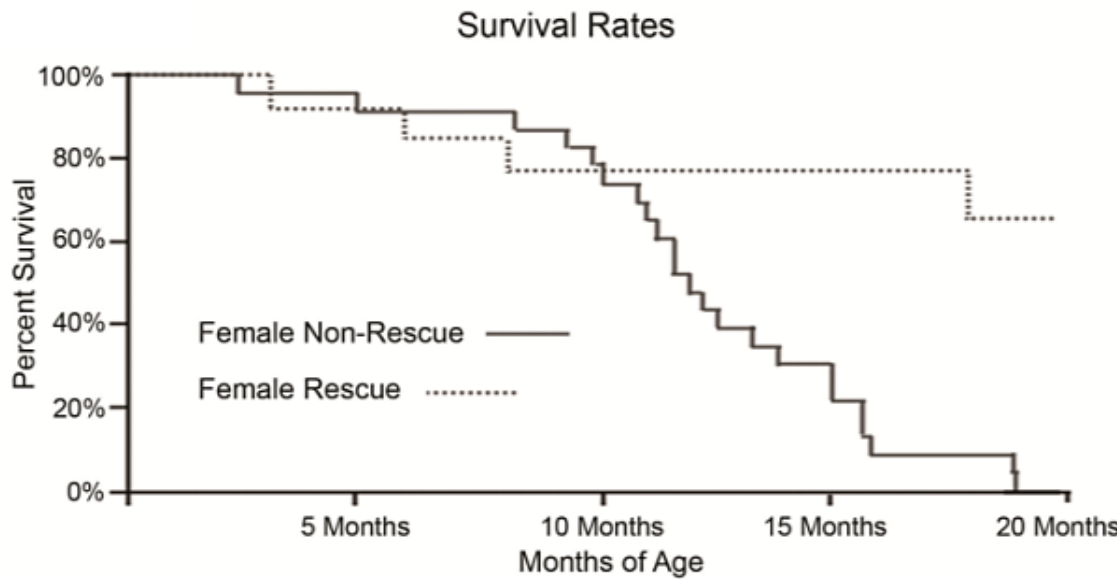


Mecp2-Deficient Mice

Mecp2 Gene
Reactivation



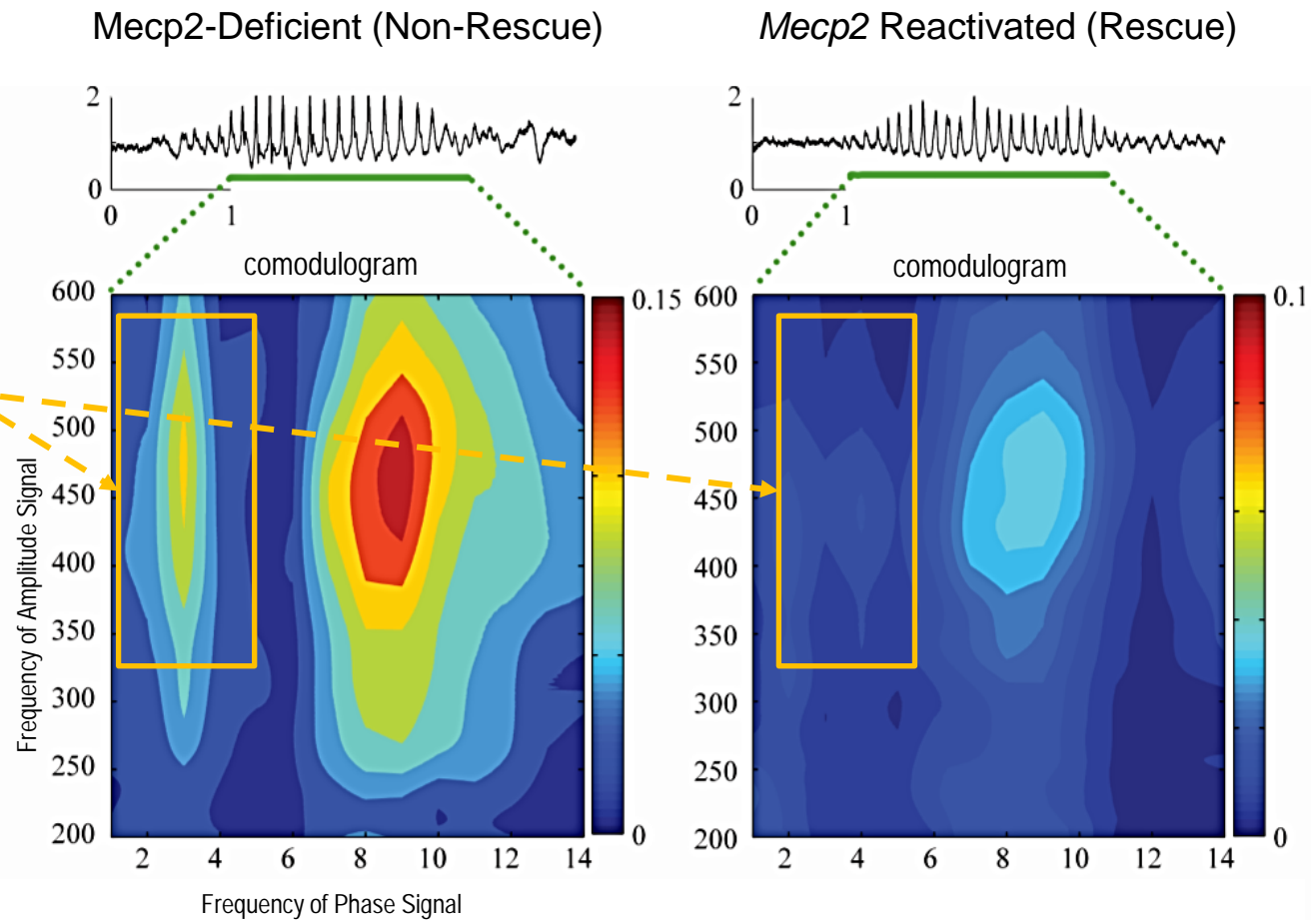
Rescue Mice



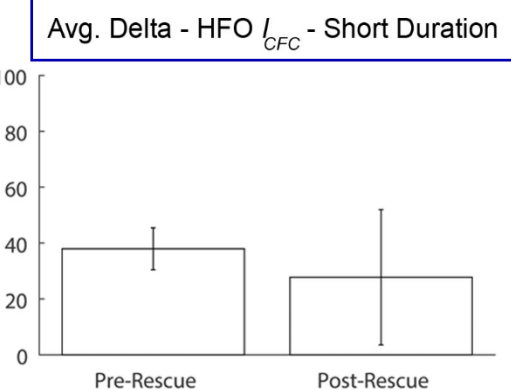
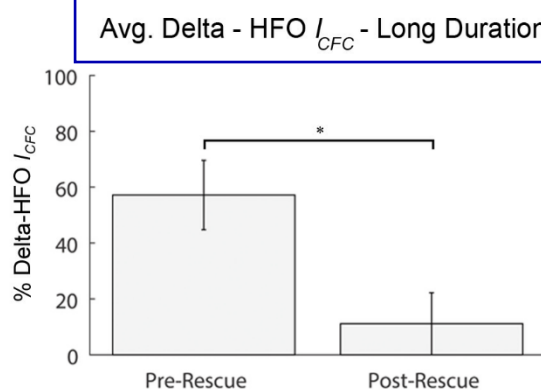
- *Mecp2* gene reactivation increases lifespan
- Improvements observed in behavioural scores [Lang et al., 2013]
- *Mecp2* deficiency can be treated

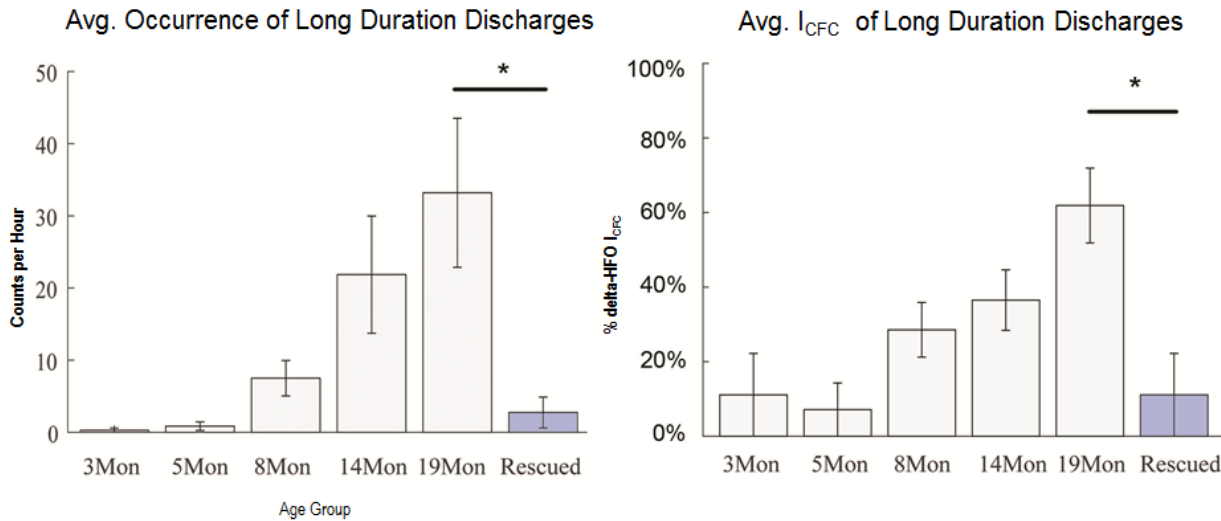
I_{CFC} Post *Mecp2* Gene Reactivation

**Delta-HFO is
greatly reduced
after *Mecp2* gene
reactivation**



I_{CFC} Pre- and Post- Rescue

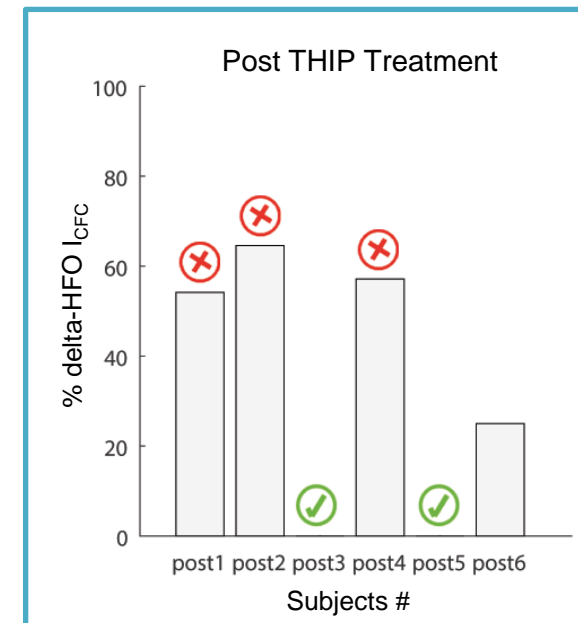
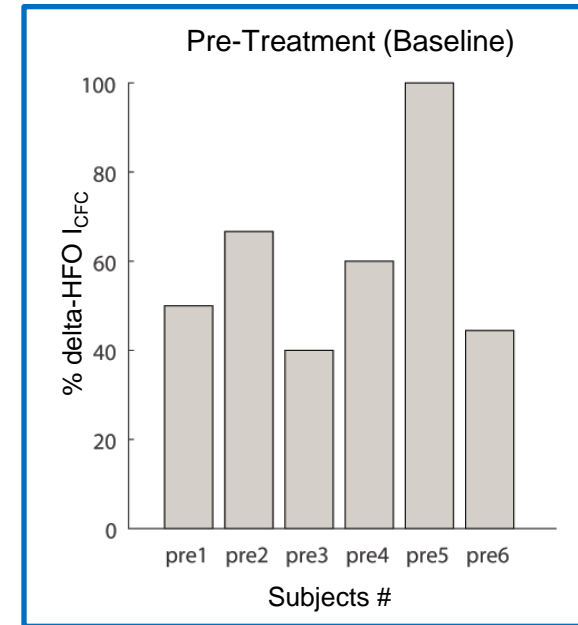
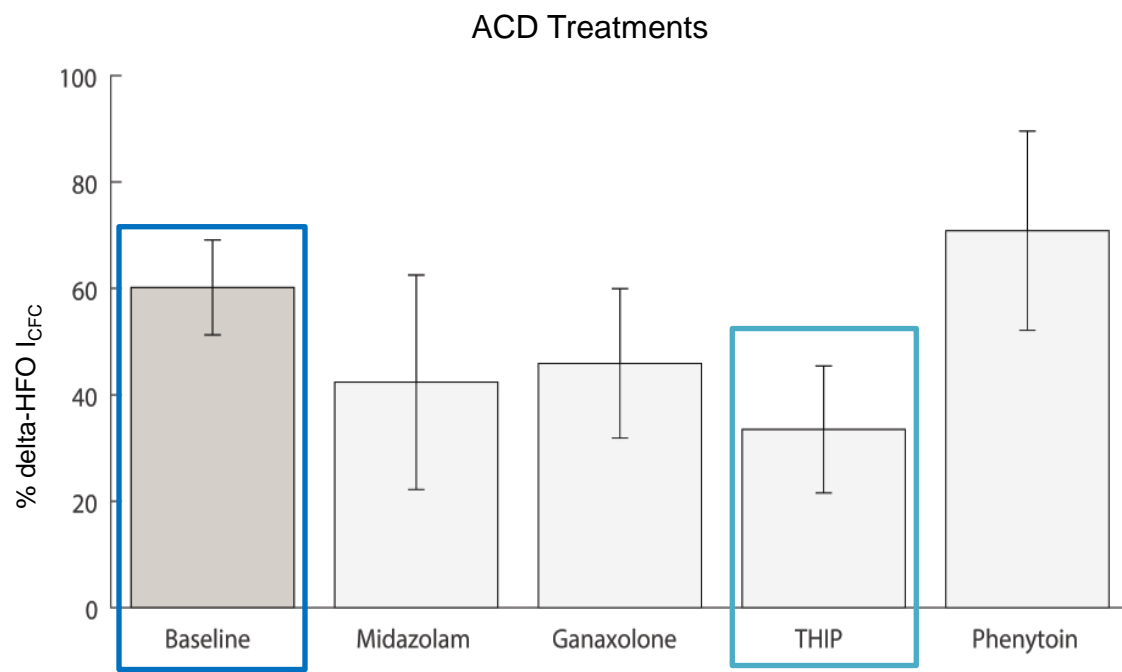




- Long duration epileptiform discharges are reduced post *Mecp2* gene reactivation
- Delta-HFO I_{CFC} is minimized post *Mecp2* gene reactivation

Anticonvulsants Drug (ACD) Treatment Outcomes

- Examined presence of delta-HFO (2-5 Hz with 400-600 Hz) I_{CFC} in long duration discharges post drug treatment in ($n=6$) Mecp2-deficient mice
- Averages could be misleading



Treatment Outcomes

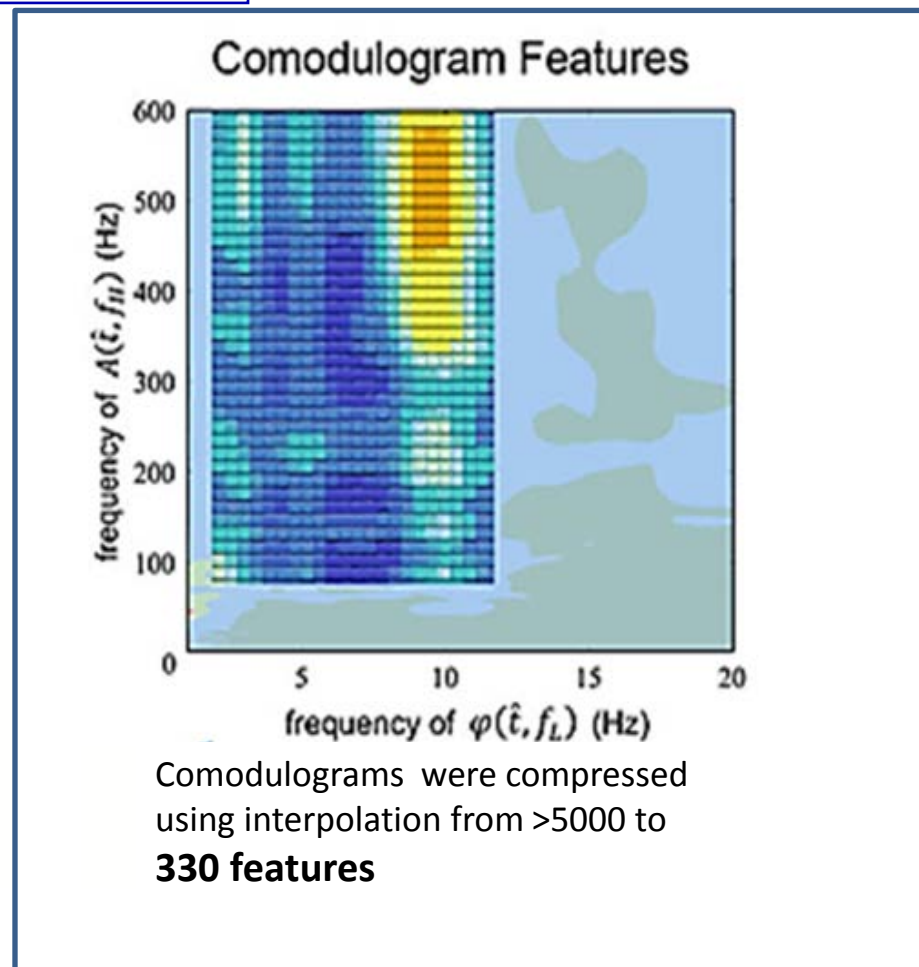
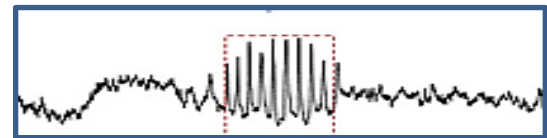
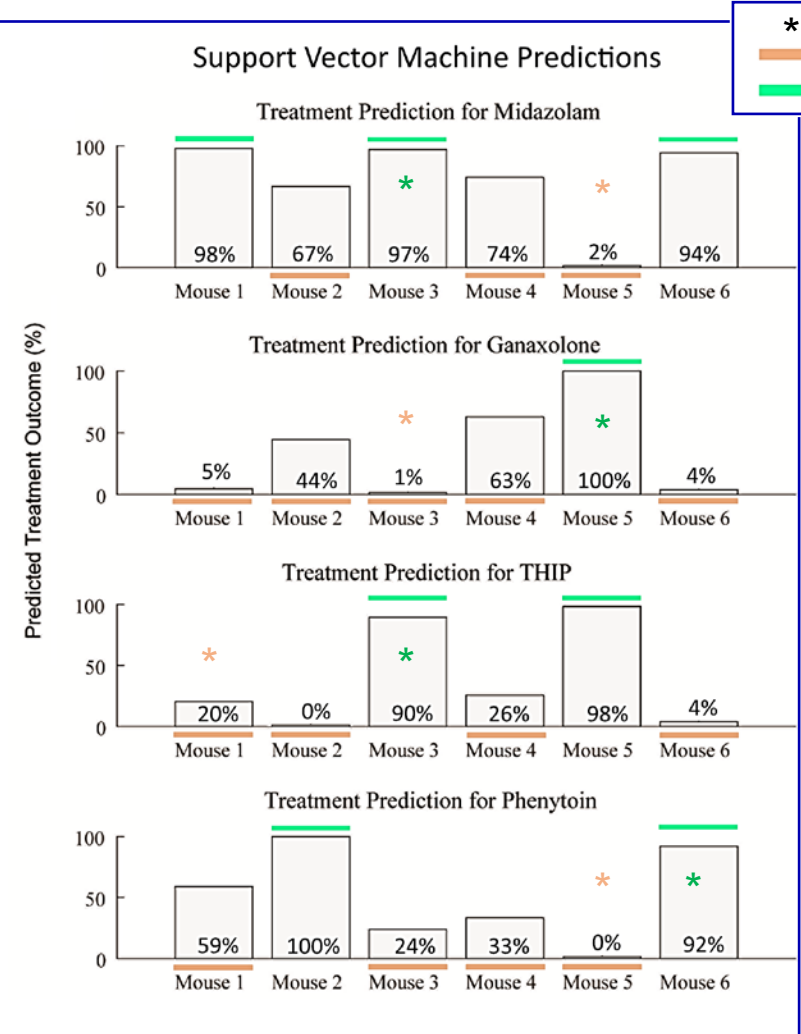
- Responder and non-responder labels (25% used as threshold)
- Variability of treatment response observed across subjects

	Percentage of delta-HFO I_{CFC} across animals subjects						Avg.
BASELINE	50	67	40	60	100	44	60
MID	0	54	0	100	100	0	42
GAN	33	69	100	38	0	35	46
THP	54	65	0	57	0	25	33
PHE	100	0	100	100	100	25	71

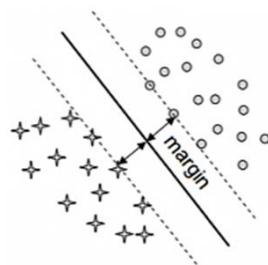


Prediction of Treatment Outcome

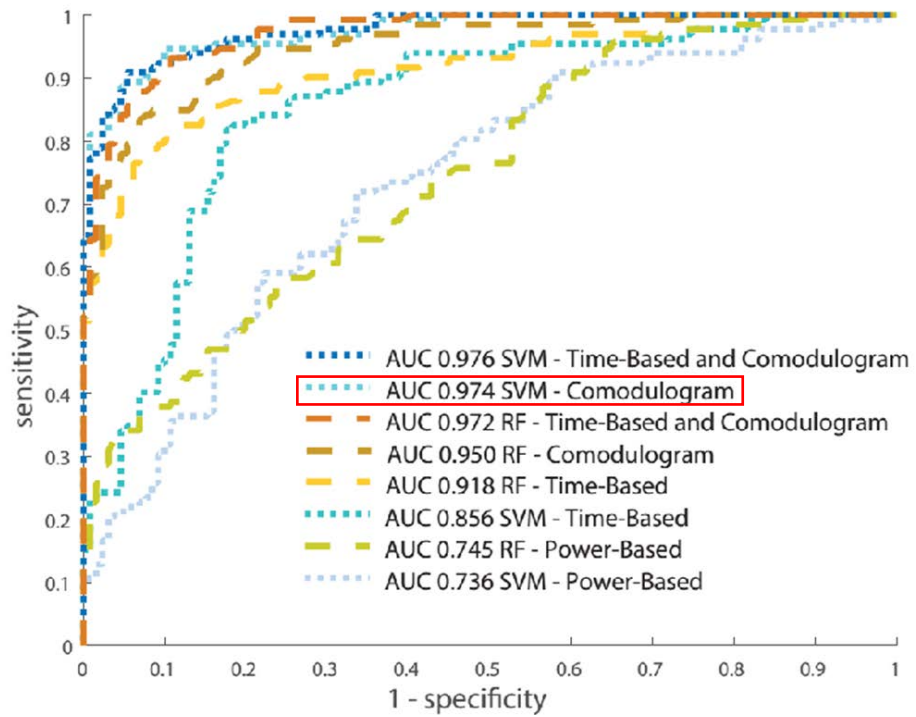
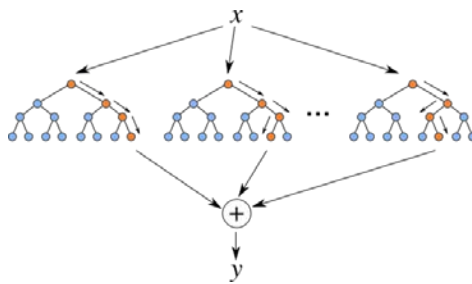
SVM prediction of successful treatment outcome closely matches post ACD treatment outcome.

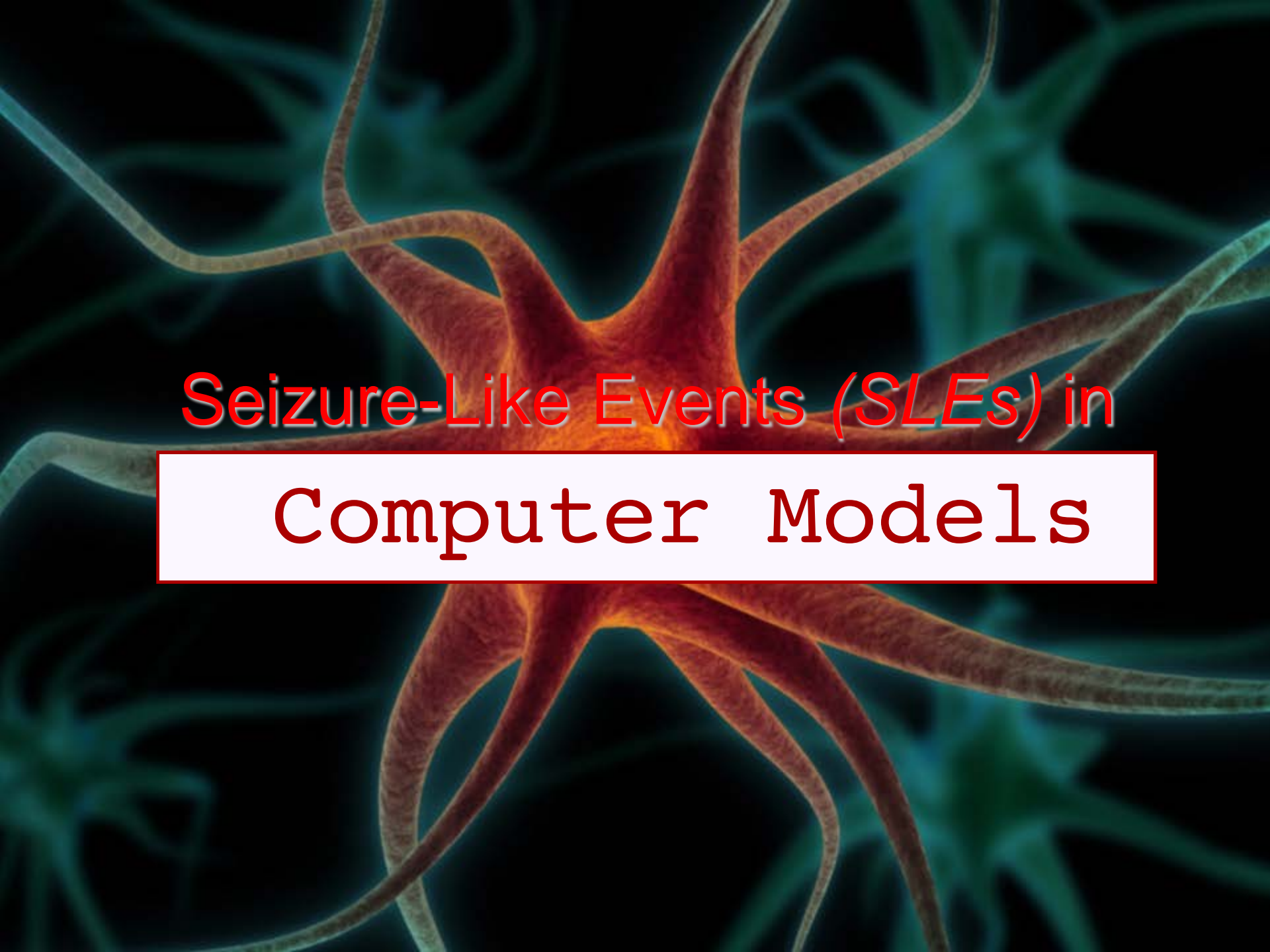


Support Vector Machine (SVM)



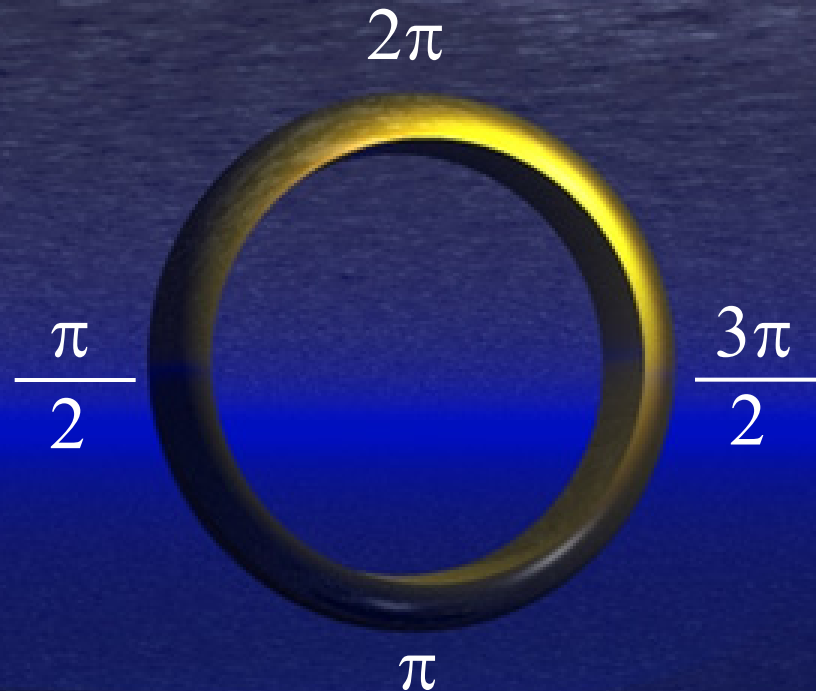
Random Forest (RF)





Seizure-Like Events (*SLEs*) in Computer Models

Ring Devices

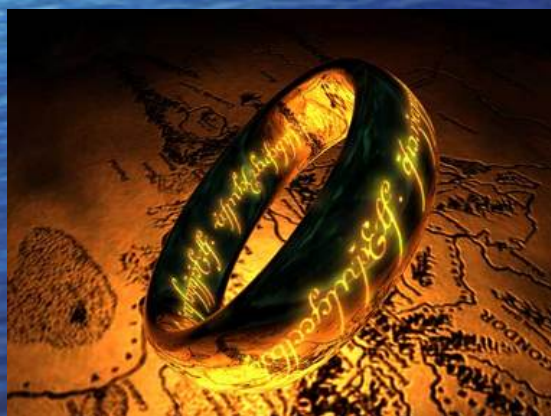


A continuum of states is represented as real numbers $(0, 2\pi]$

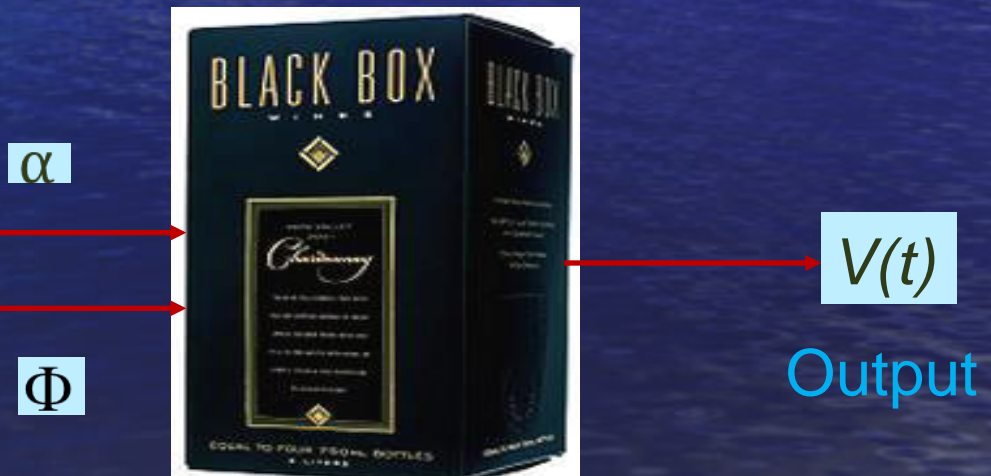
Arthur Winfree proposed **ring devices** to describe amplitude and phase dynamics to characterize intrinsic biological rhythms.

Rhythm Generators

- The dynamics of Ring Devices are described in terms of phase and amplitude.
- Changes in phase or amplitude reflect changes in state.
- The instantaneous state can be ‘mapped’ to a physical quantity, such as voltage, using a **static nonlinearity**.



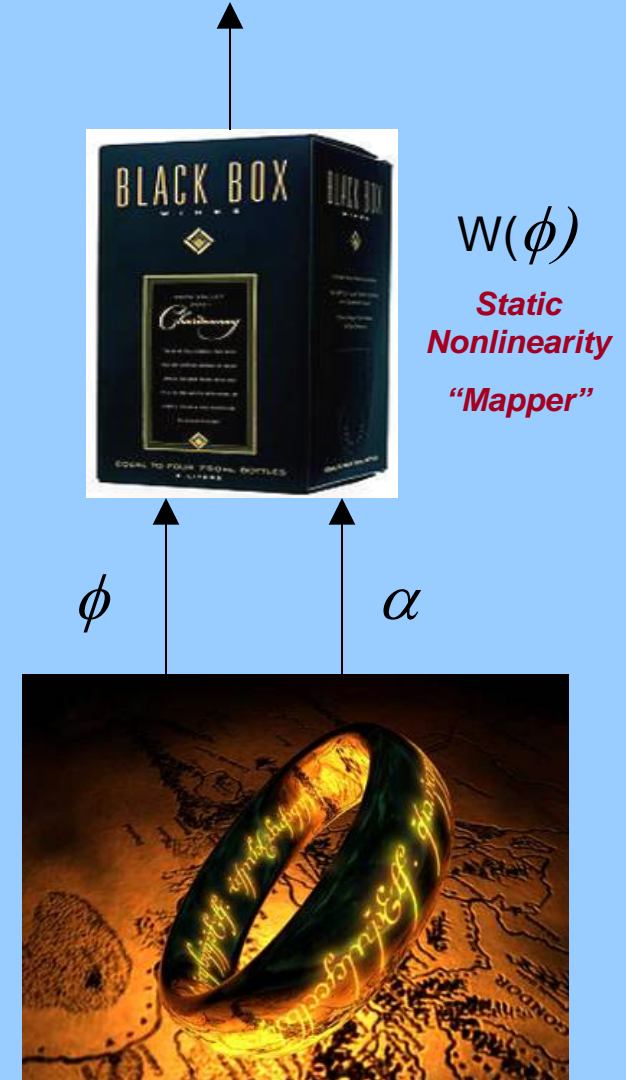
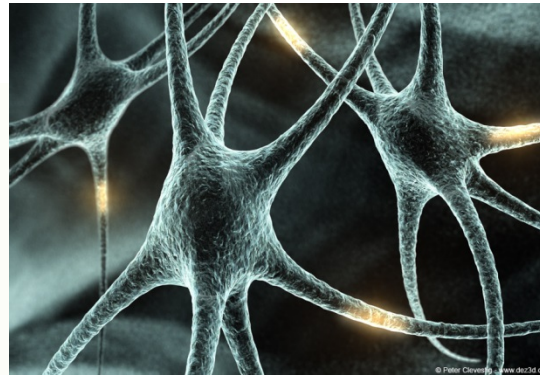
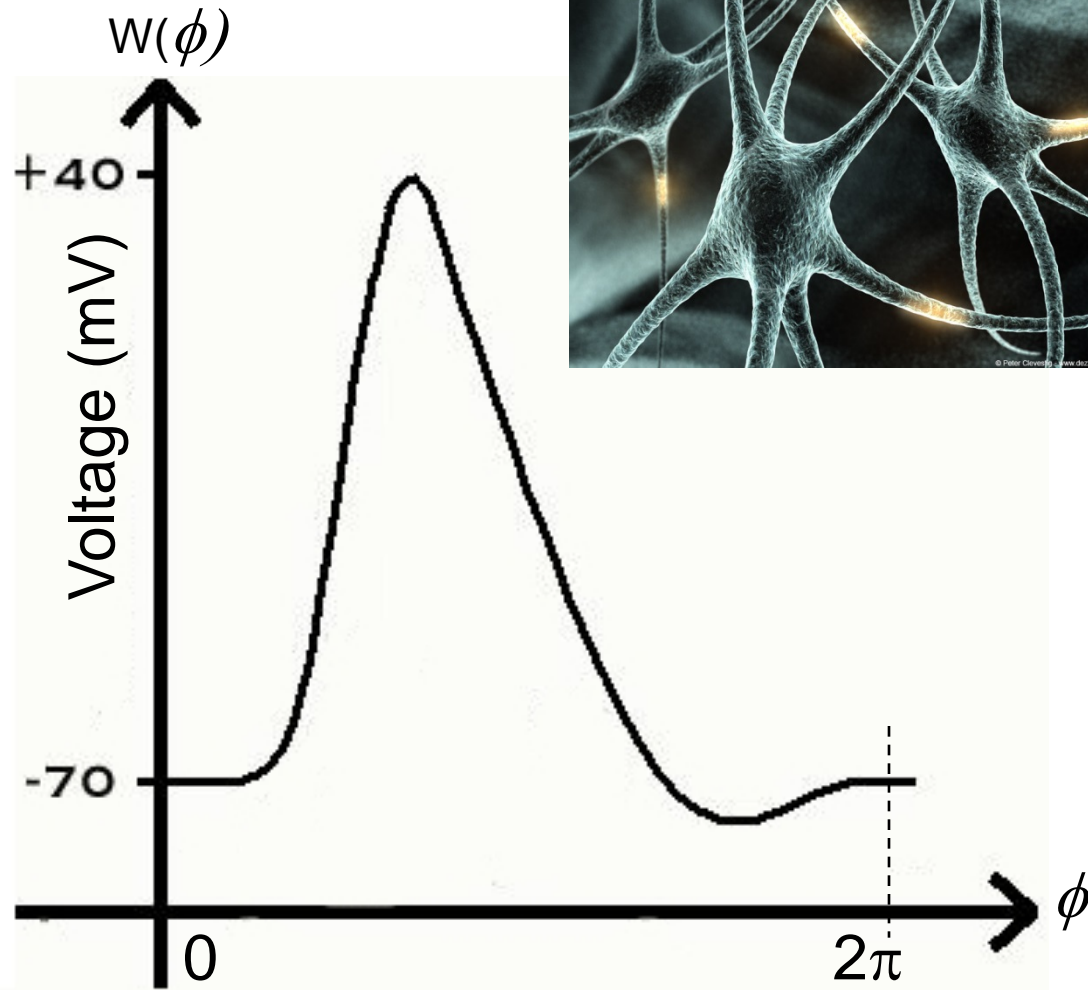
Ring Device
(dynamic ring of states)



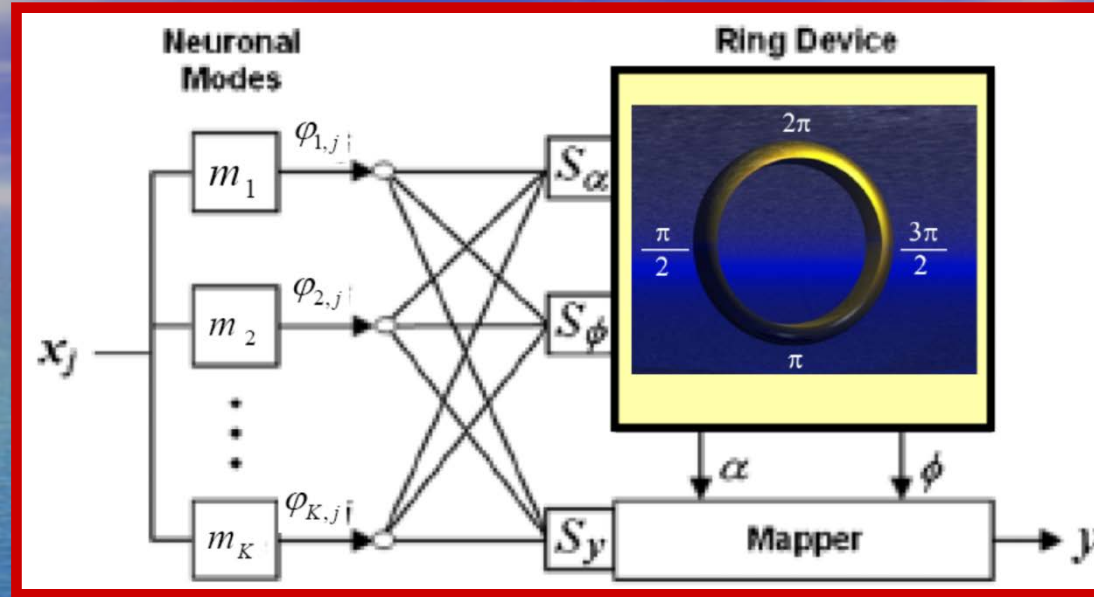
Mapper

Neural Rhythms

The action potential as a cycle



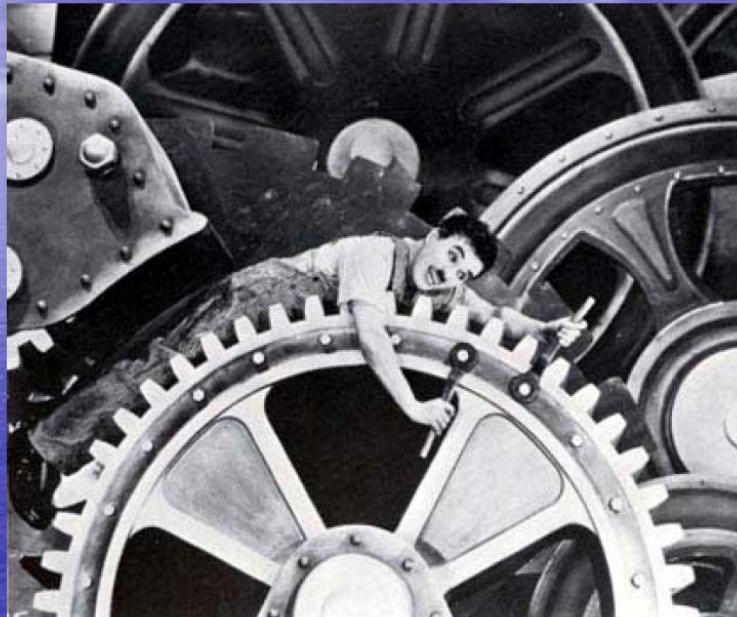
Cognitive Rhythm Generators (CRGs)



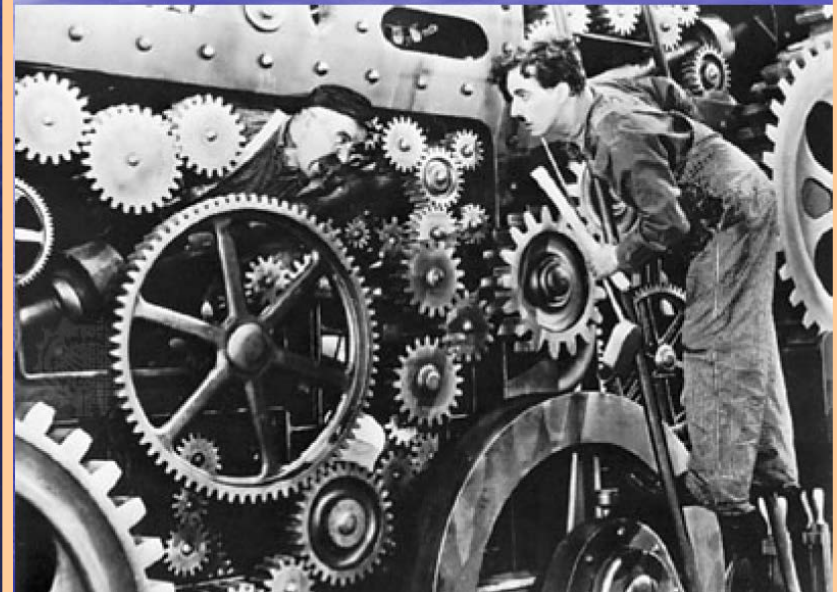
- The **cognitive aspect** of the **CRG** derives from input decoding performed by an orthogonal set of neuronal modes representing the system kernels. **Cognition** involves both **perception** and **information processing**, so the modes provide the medium through which the **CRG** perceives its environment and performs an initial transformation of the incoming signals.
- The rhythm generator takes the mode-transformed signals and encodes them into amplitude and phase variables that are then mapped to an observable output by a static nonlinearity.



Ring Parameters can be adjusted



Rings can be coupled



Fellowship of the Rings



A Dynamic “Intermittency” Perspective of Epilepsy



Ictal and Interictal Events
are embedded in the
Higher Complexity Ring
formed by the coupled rings

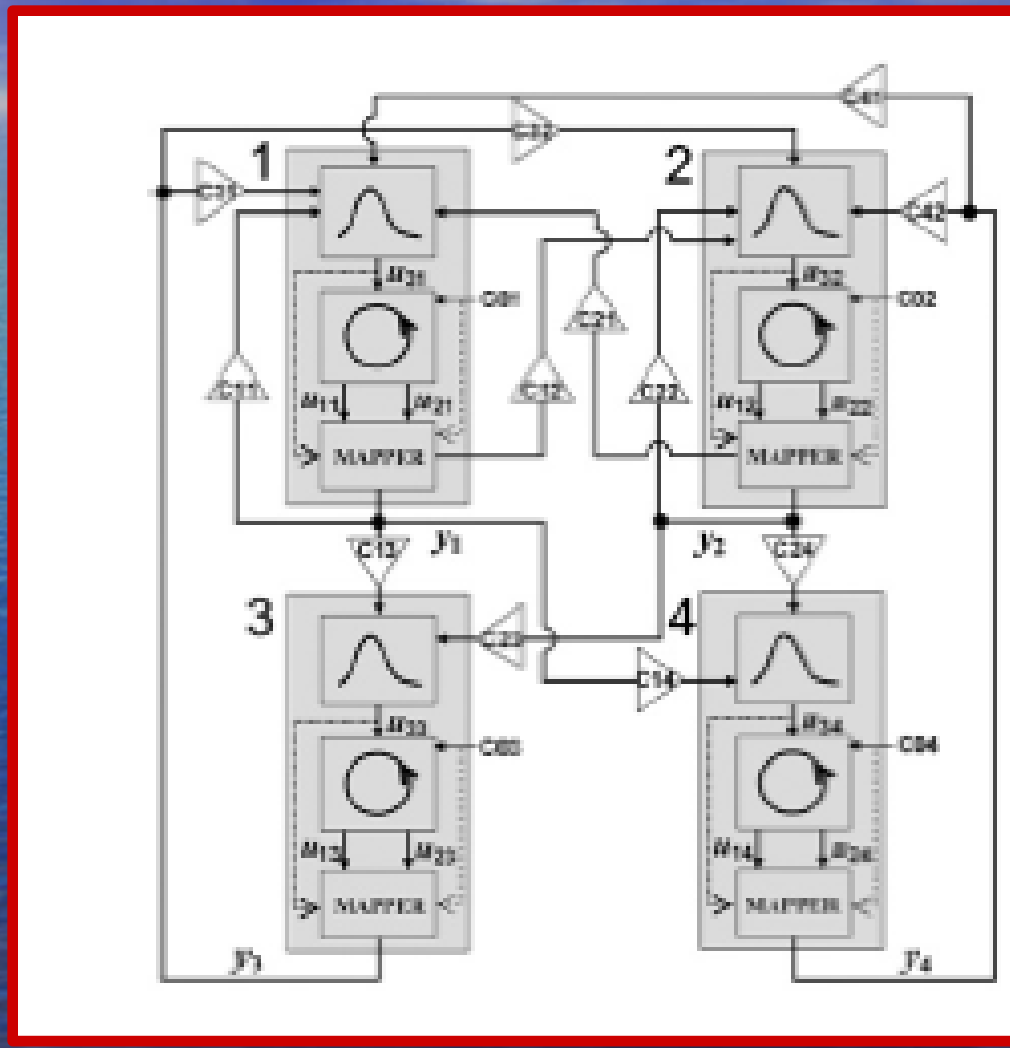


System characterization of neuronal excitability in the hippocampus and its relevance to observed dynamics of spontaneous seizure-like transitions

Osbert C Zalay¹, Demitre Serletis^{1,2,3}, Peter L Carlen^{1,2,3} and
Berj L Bardakjian^{1,4}



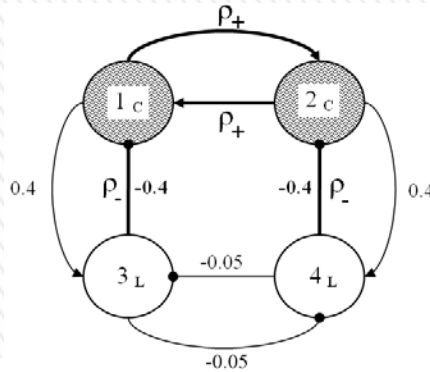
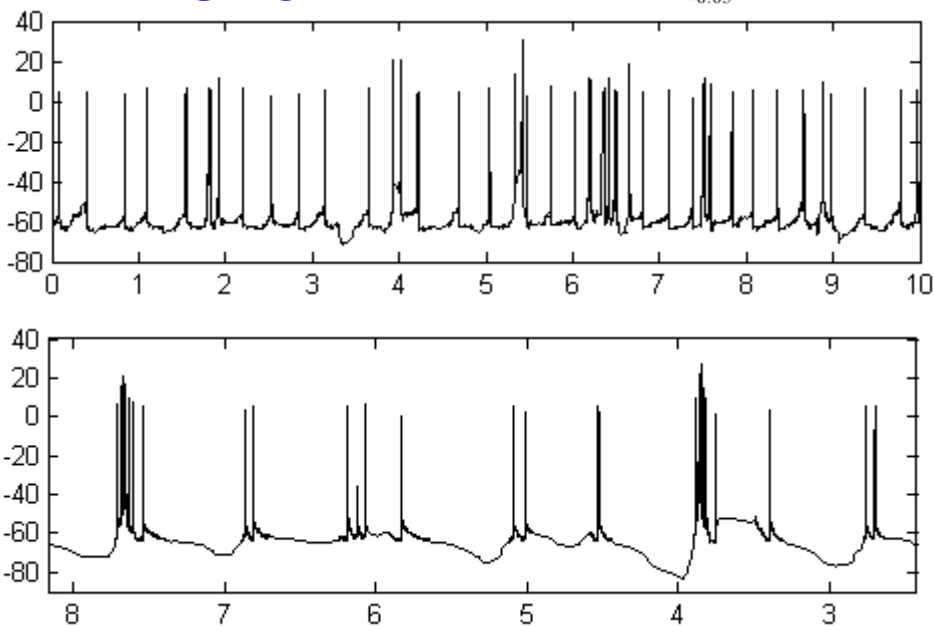
Model of spontaneous SLEs using 4 Coupled CRGs



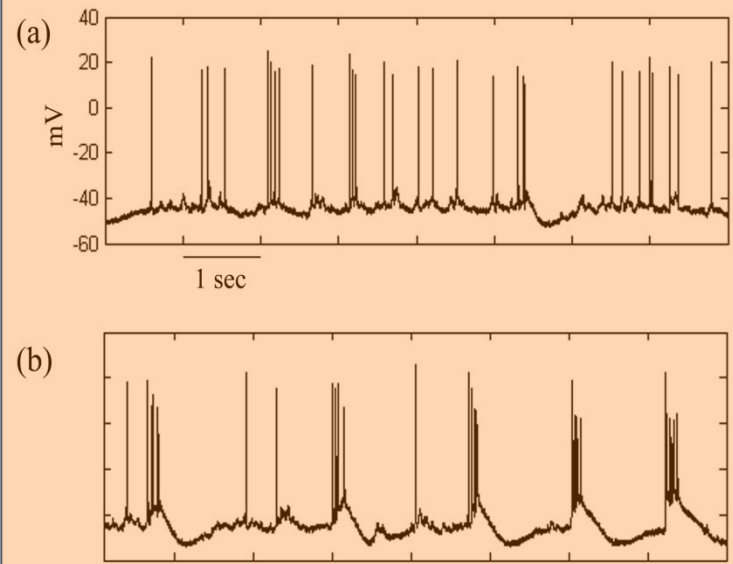
Simulating Neuronal Dynamics

» CRGs can generate outputs with [waveforms](#) and rhythms that have similar properties and complexity to those produced by biological neural networks

CRG network model of hippocampal CA3

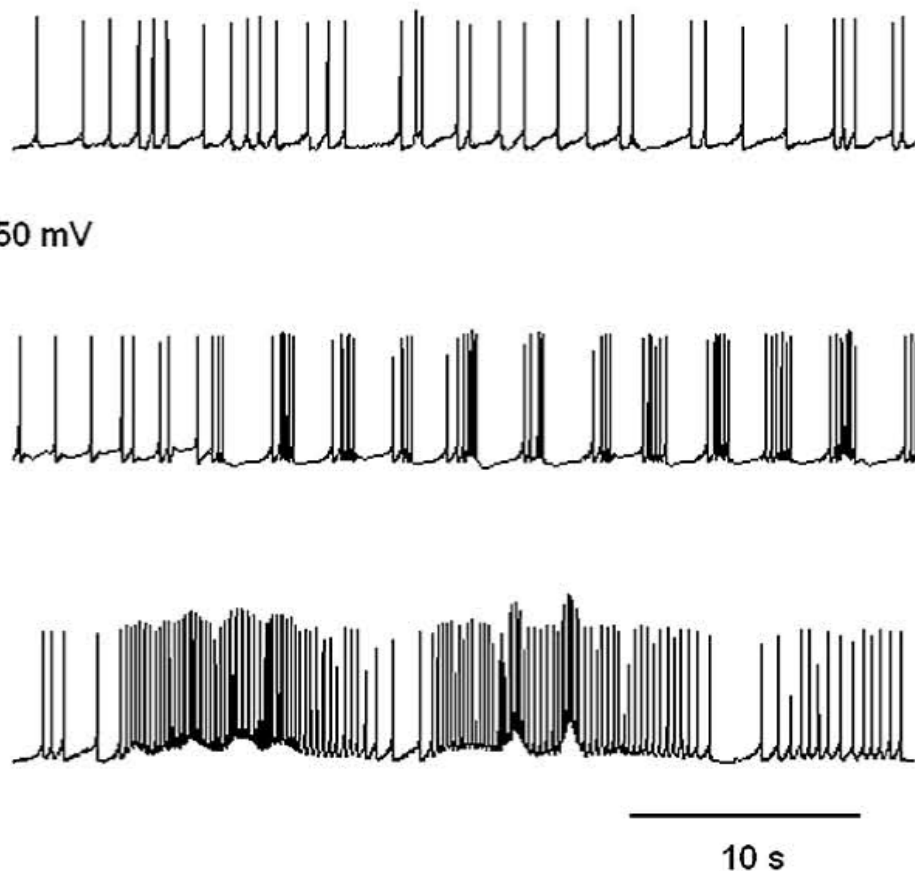


Intracellular recording (CA3 region – hippocampal slice under low Mg^{2+})



CRG Model of Spontaneous SLEs

Decreasing Mode Decay Rate (*increasing excitability*)



$$\beta = 2$$

LFP



CRG 1



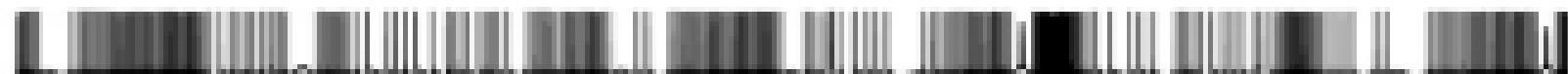
CRG 2



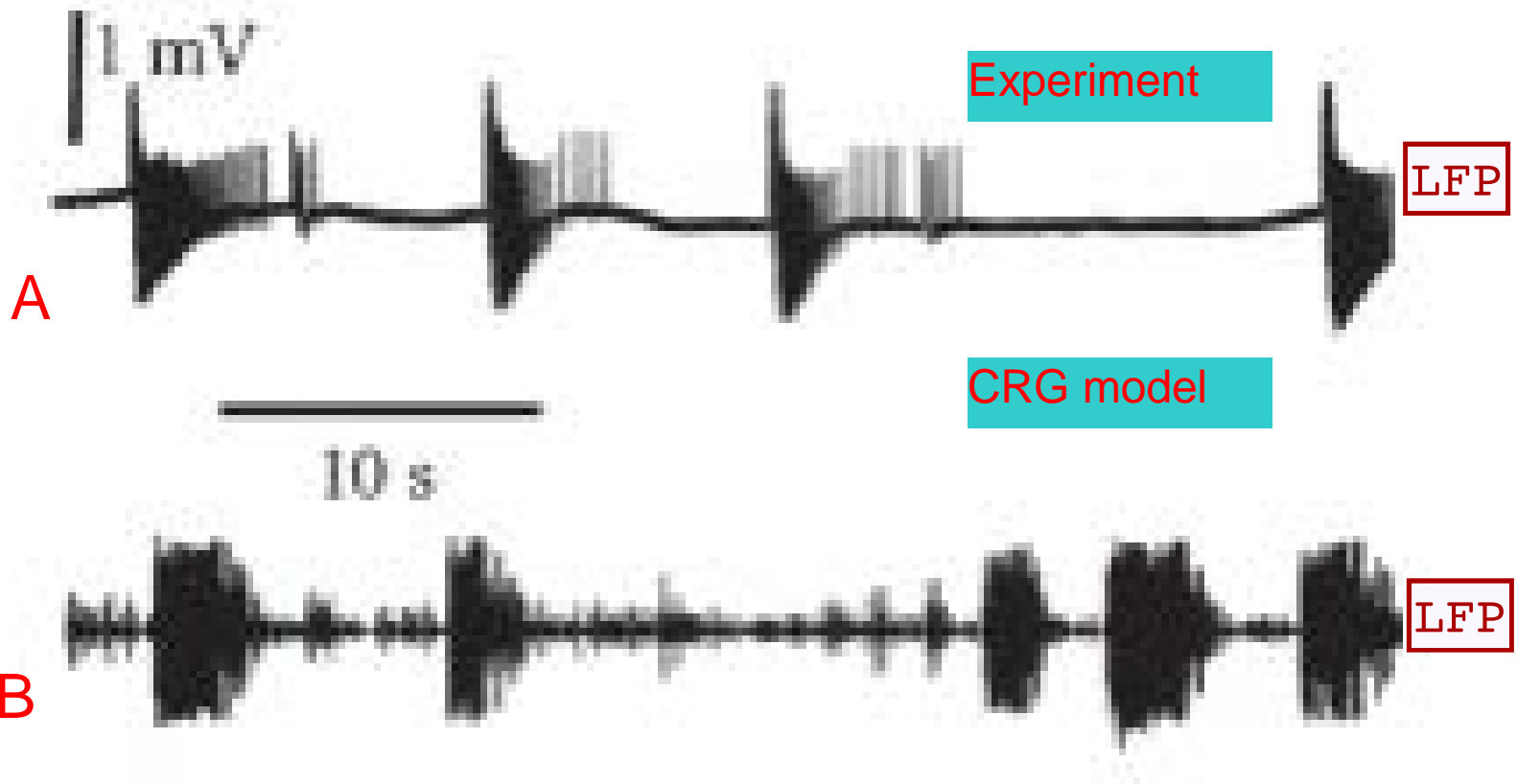
CRG 3



CRG 4



10 s



Extracellular field recording showing recurrent SLEs from
(A) *stratum pyramidale* in a rat hippocampal slice, and
(B) CRG model. The experimental trace was de-trended.



Brain stimulation strategies to stop seizures

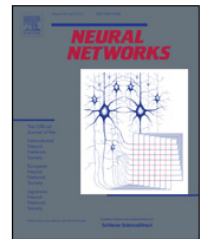


ELSEVIER

Contents lists available at SciVerse ScienceDirect

Neural Networks

journal homepage: www.elsevier.com/locate/neunet



Synthesis of high-complexity rhythmic signals for closed-loop electrical neuromodulation

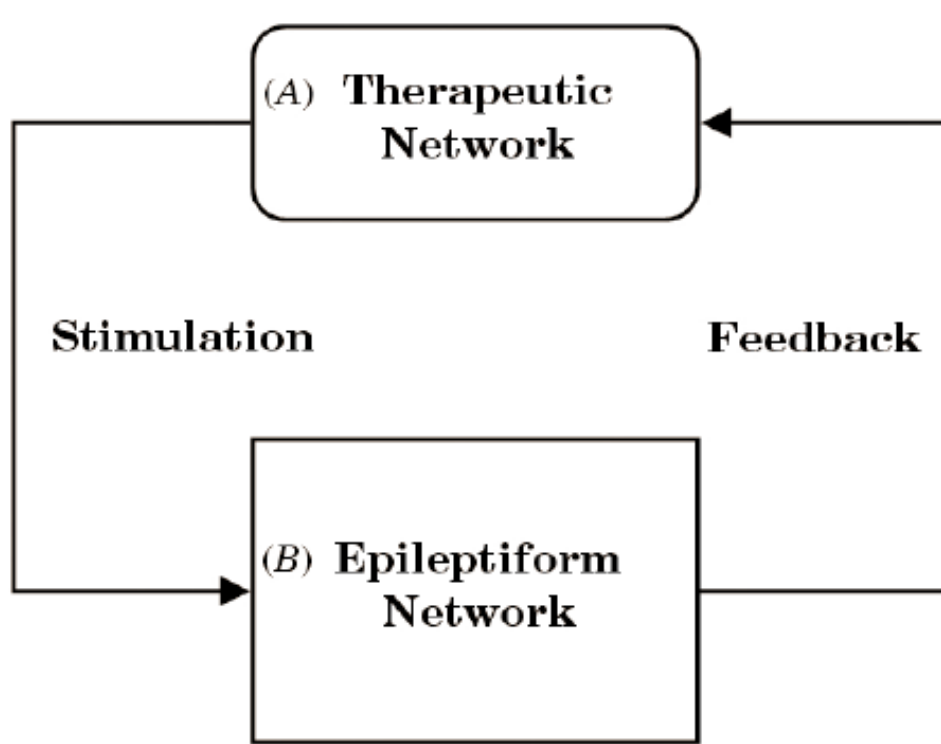
Osbert C. Zalay*, Berj L. Bardakjian

Institute of Biomaterials and Biomedical Engineering, University of Toronto, 164 College Street, Toronto, Ontario, M5S 3G9, Canada



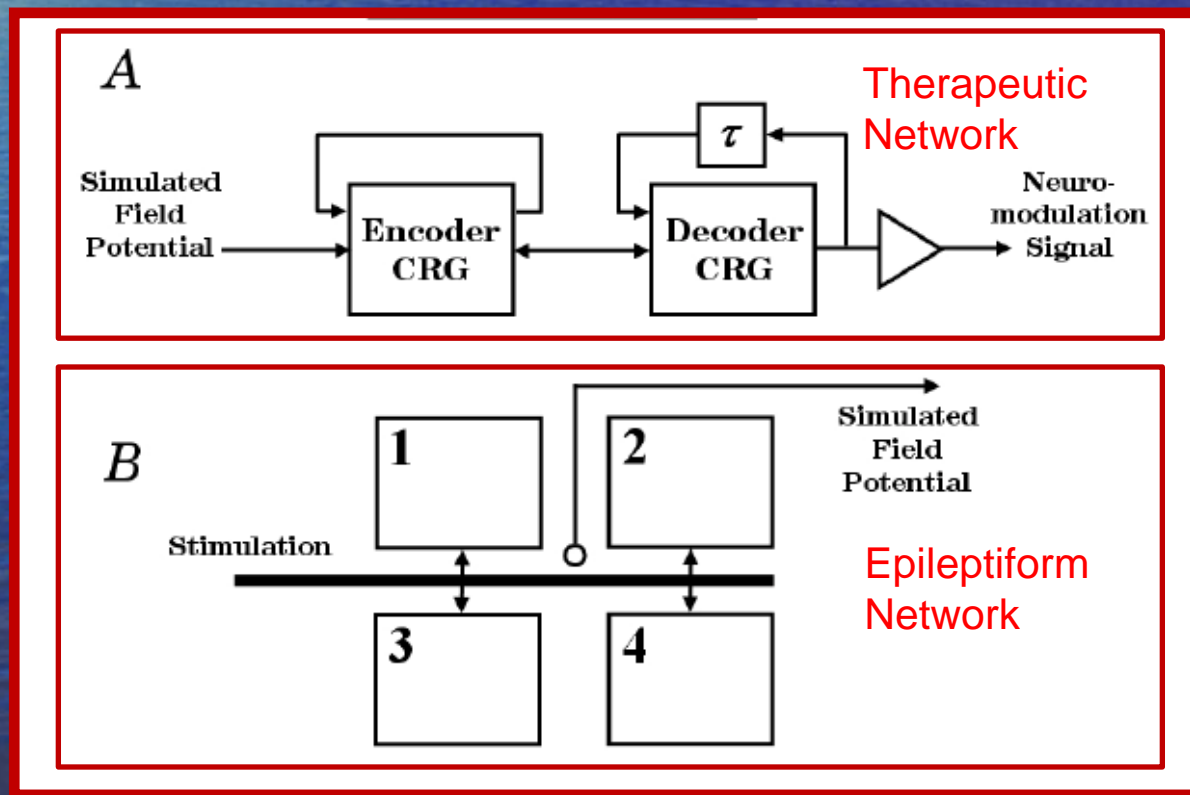
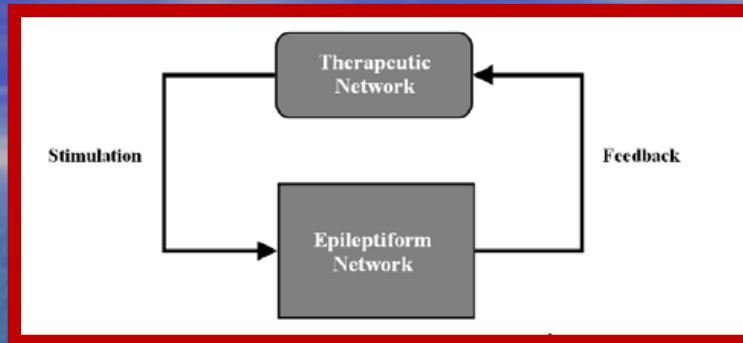
CRG Network Neuromodulation

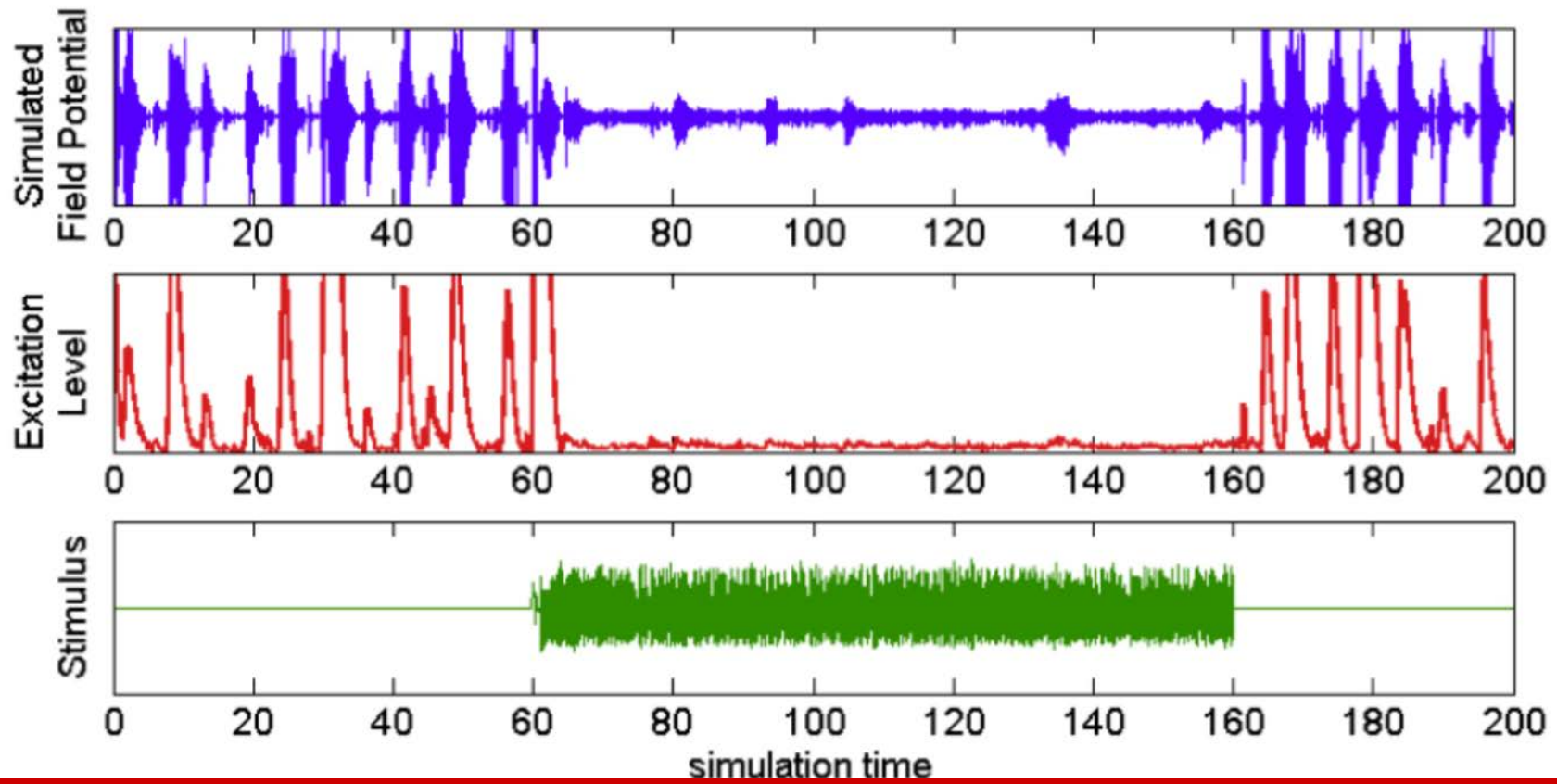
Interface therapeutic network with the CRG intermittent SLE network



Strategy: High-complexity (neuromimetic), closed-loop modulation of SLE network activity for **seizure suppression** and **restoration of high dynamic complexity**

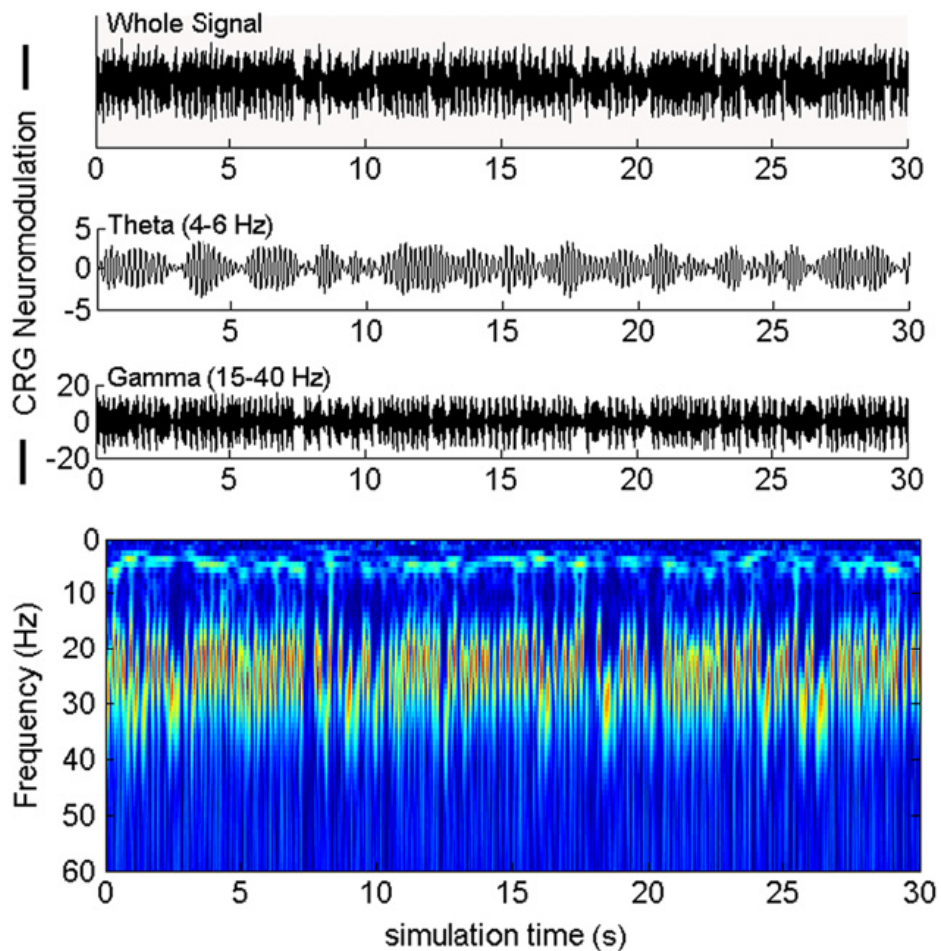
Therapeutic & Epileptiform Networks





In a **computer model of spontaneous SLEs using 4 coupled CRGs**, an optimal control system was designed using the pattern search method where the **therapeutic network consisting of 2 CRGs (Encoder and Decoder)** was tuned by minimizing a cost function which was the weighted sum of (a) the total time spent seizing, (b) seizure duration, and (c) the stimulation energy. This provided a responsive therapeutic stimulation which, when activated, **completely blocked seizure activity** in an epileptiform network.

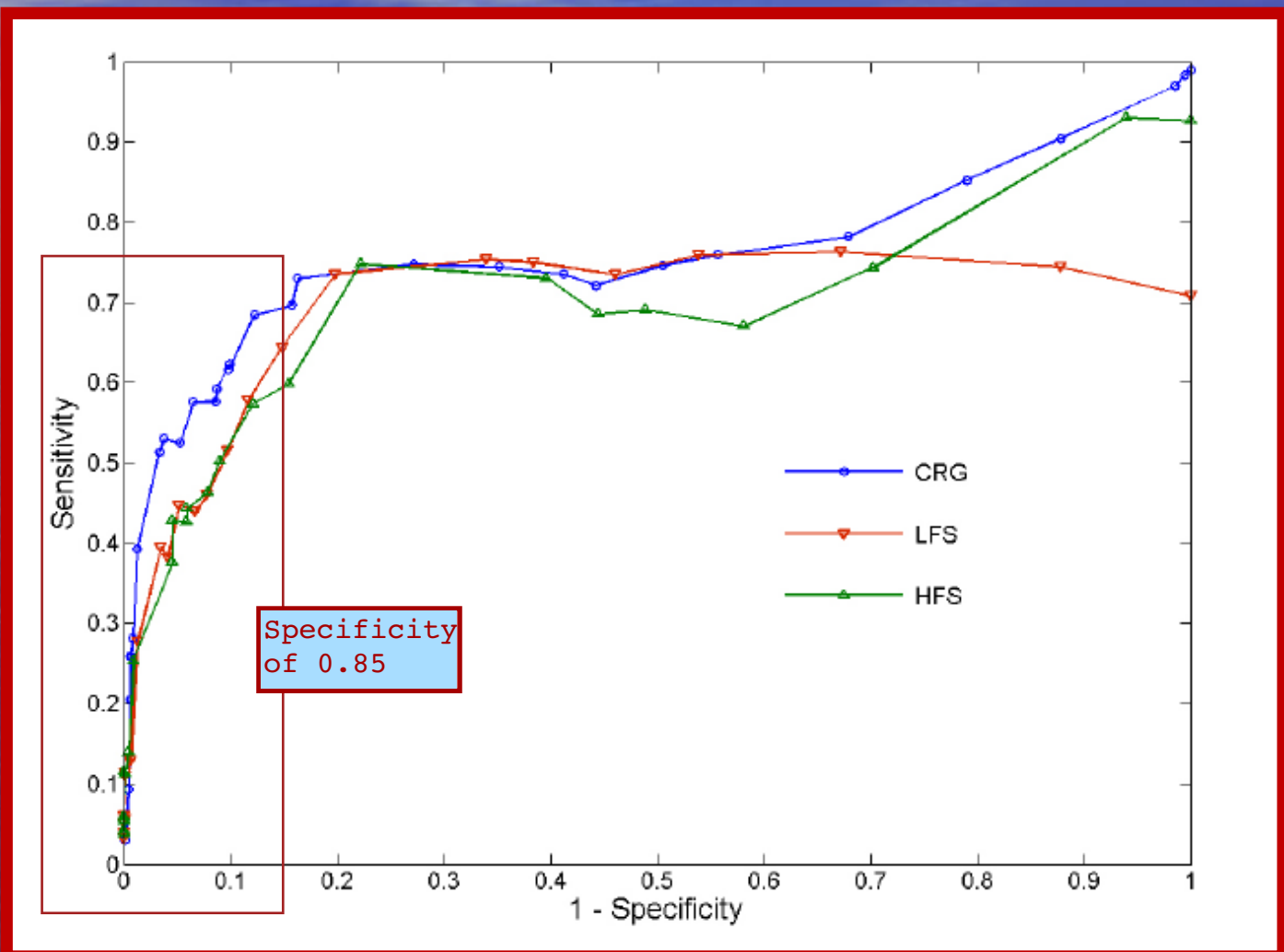
The characteristics of the optimal stimulation for seizure suppression inherent in the neuromodulation stimulus. Note the polyrhythmic nature (Theta and Gamma) of this complex efficacious stimulus, as compared to the periodic stimulations currently used with success in deep brain stimulation for epilepsy.



Dynamic complexity of neuromodulation stimulus (mean \pm std. dev.).

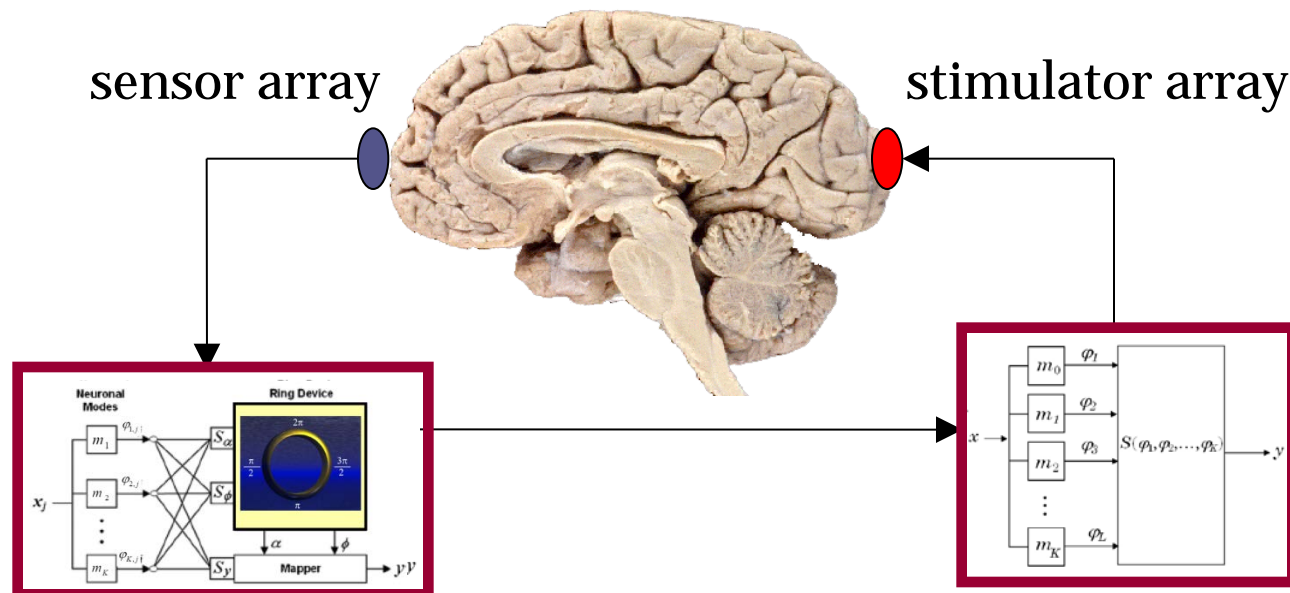
Complexity measure	Theta (4–6 Hz)	Gamma (15–40 Hz)	Whole signal
Max. Lyapunov exp. (bits/s)	1.28 ± 0.37	1.00 ± 0.38	-
Correlation dim.	3.64 ± 0.12	5.20 ± 0.29	>6

Receiver Operating Characteristic (ROC) Curves of Neuromodulation by CRG, periodic LFS (10 Hz) and periodic HFS (120 Hz) Paradigms.

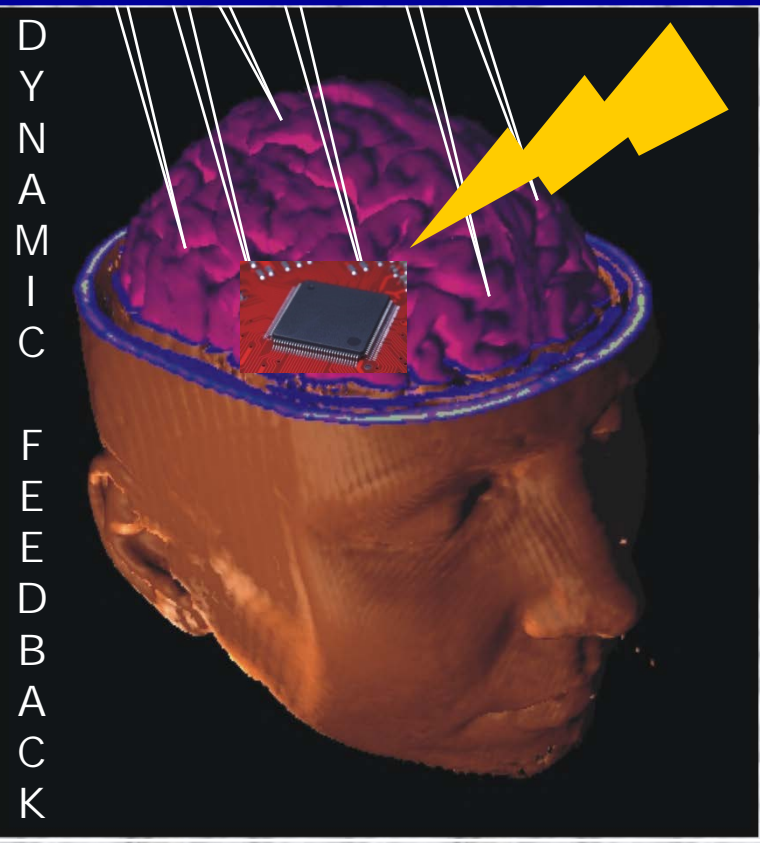


Seizure Abolishment Strategy

- A *responsive neuromodulator* can be designed to prevent seizure-like events in animal epilepsy models (in-vitro and in-vivo) and possibly in human patients



Cognitive Brain Device



Theta phase precession and phase selectivity: a cognitive device description of neural coding

Osbert C Zalay and Berj L Bardakjian

J. Neural Eng. 7 (2010) 036002 (15pp)

doi:10.1088/1741-2560/7/3/036002

System characterization of neuronal excitability in the hippocampus and its relevance to observed dynamics of spontaneous seizure-like transitions

Osbert C Zalay¹, Demitre Serletis^{1,2,3}, Peter L Carlen^{1,2,3} and Berj L Bardakjian^{1,4}

Neural Networks 42 (2013) 62–73



ELSEVIER

Contents lists available at SciVerse ScienceDirect

Neural Networks

journal homepage: www.elsevier.com/locate/neunet



Synthesis of high-complexity rhythmic signals for closed-loop electrical neuromodulation

Osbert C. Zalay*, Berj L. Bardakjian

Institute of Biomaterials and Biomedical Engineering, University of Toronto, 164 College Street, Toronto, Ontario, M5S 3G9, Canada

